# Novel methods for assessing left ventricular dyssynchrony and myocardial function

**PhD thesis 2012**

**Kristoffer Engh Russell**

**Department of Cardiology and**
**Institute for Surgical research,**
**University of Oslo**
**Oslo University Hospital,**
**Rikshospitalet**

*Series of dissertations submitted to the*
*Faculty of Medicine, University of Oslo*
*No. 1422*

ISBN 978-82-8264-397-9



Cover: Inger Sandved Anfinsen.
Printed in Norway: AIT Oslo AS.

Produced in co-operation with Akademika publishing.
The thesis is produced by Unipub merely in connection with the
thesis defence. Kindly direct all inquiries regarding the thesis to the copyright
holder or the unit which grants the doctorate.

# Acknowledgments

The present work was carried out at the department of cardiology, Institute of surgical research, Oslo university Hospital, Rikshospitalet, from October 2008 to December 2011.
I have been privileged to have one of the world's foremost authorities on heart physiology and mechanics as my supervisor. Prof. Otto A. Smiseth possesses a vast and impressive knowledge of pathophyiology of the heart. Otto has introduced me to heart mechanics and experimental research while always emphasising the importance of clinical relevance. His enthusiasm and hard work has served as tremendous encouragement. Despite his busy schedule as head division of cardiovascular and pulmonary diseases, he has always found time for research and discussion.
Prof. Thor Edvardsen has been in the forefront of echocardiography and cardiac imaging research and is internationally renowned for his work. Thor possesses a unique ability to motivate and encourage and I have found his advice and comments to be invaluable. As my co supervisor Thor introduced me to echocardiography and measurements such as strain, statistical analysis and much more. His door has always been open, something I have often taken advantage of.
The clinical aspects of my thesis would not have been possible without the support of the department of cardiology and its head, Lars Aaberge. Lars also played a central part in the clinical study together with Nils Wilhelmsen and I would like to thank them and the rest of the staff in the cath lab for their support. I would also like to thank Prof. Ansgard Aasen for office facilities and a stimulating research environment at the Institute for Surgical Research.
I would also like to thank my fellow researchers Anders Opdahl, Espen W. Remme, Helge Skulstad, Morten Eriksen, Ola Gjesdal, Kristina Haugaa and Espen Bøe for their support, genuine interest and friendship. This would not have been possible without you.
I am grateful to the University of Oslo for their research fellowship and for support from the Inger and John Fredriksen fund.
Finally I would like to thank my family. My parents Grete and David for always believing in me and supporting me. I would also like to thank my parents' partners Aage and Jeanette and my parents in law Sybille and Sean for their encouragement. Most importantly, my thanks and love goes to my beautiful wife Hannah who has given me unfailing support and who makes it all worth while.

# Abbreviations

| | |
|---|---|
| LV | Left ventricle |
| STE | Speckle tracking echocardiography |
| CRT | Cardiac resynchronization therapy |
| LBBB | Left bundle branch block |
| TDI | Tissue Doppler imaging |
| IM-EMG | Intramyocardial electromyograms |
| AFG | Active myocardial force generation |
| EMD | Electromechanical delay |
| REA | Regional electrical activation |
| OS | Onset of shortening |
| IVC | Isovolumic contraction |
| IVR | Isovolumic relaxation |
| FDG-PET | 18F-fluorodeoxyglucose positron emission tomography imaging |
| WWF | Wasted work fraction |

# List of papers

1. **Evaluation of left ventricular dyssynchrony by onset of active myocardial force generation - a novel method which differentiates between electrical and mechanical etiologies**
Kristoffer Russell; Anders Opdahl; Espen W. Remme; Ola Gjesdal; Helge Skulstad; Erik Kongsgaard; Thor Edvardsen; Otto A. Smiseth.
Circ Cardiovasc Imaging. 2010 Jul 1;3(4):405-14

2. **Mechanism of Prolonged Electro-Mechanical Delay in Late Activated Myocardium during Left Bundle Branch Block**
Kristoffer Russell; Otto A. Smiseth; Ola Gjesdal; Eirik Qvigstad; Per Andreas Norseng; Ivar Sjaastad; Anders Opdahl; Helge Skulstad; Thor Edvardsen; Espen W. Remme.
Am J Physiol Heart Circ Physiol. 2011 Dec;301(6):H2334-43. Epub 2011 Oct 7.

3. **A novel clinical method for quantification of regional left ventricular pressure-strain area – a noninvasive index of segmental work**
Kristoffer Russell; Morten Eriksen; Lars Aaberge; Nils Wilhelmsen; Helge Skulstad; Anders Opdahl; Espen W. Remme; Kristina Herman Haugaa; Thor Edvardsen; Otto A. Smiseth.
Eur Heart J. 2012 Mar;33(6):724-33. Epub 2012 Feb 6.

4. **Wasted work fraction – A novel method for quantifying left ventricular function.**
Kristoffer Russell; Morten Eriksen; Lars Aaberge; Nils Wilhelmsen; Helge Skulstad; Ola Gjesdal; Thor Edvardsen; Otto A. Smiseth.
Submitted

# Introduction

## Dyssynchrony in the heart

In the normal heart electrical activation spreads rapidly throughout the ventricles through the specialized conduction system, resulting in a synchronous ventricular contraction. In some patients this conduction system is damaged resulting in a slower spread of electrical activation from myocyte to myocyte. In the left ventricle this may result in left bundle branch block (LBBB). Patients with LBBB commonly demonstrate left ventricular (LV) mechanical dyssynchrony, and the most prominent features are early contraction of the interventricular septum and delayed contraction of LV lateral wall during the isovolumic contraction phase. This abnormal contraction pattern is due to slowing of intraventricular electrical conduction with early activation of the septum and late activation of the LV lateral wall, subsequently reducing LV function.

Dyssynchrony may be divided into inter-ventricular dyssynchrony i.e. between the right and left ventricle and intra-ventricular i.e. between different walls within the left ventricle. The relative importance of inter- and intra-ventricular dyssynchrony, however, is not entirely clear and data are somewhat conflicting regarding the clinical importance of measuring inter-ventricular dyssynchrony [1, 2]. However, most evidence suggests that interventricular dyssynchrony is not as useful in the prediction of response to cardiac resynchronization therapy (CRT) as LV intraventricular dyssynchrony [3]. In the present thesis we therefore focus on LV intra-ventricular dyssynchrony since this is known to decrease pump function and aggravate heart failure.

Intra-ventricular dyssynchrony is defined as uncoordinated regional myocardial contractions [4] and may in principle have the following etiologies; 1) Electrical conduction delay which causes non-uniform timing of myocyte depolarization (*primary electrical dyssychrony*), 2) abnormalities in excitation-contraction coupling *(excitation-contraction related dyssynchrony)*, and 3) abnormal myocardial contractility or load which cause regional delay in fiber shortening (*primary mechanical dyssychrony*). This implies that observed mechanical dyssynchrony may have electrical as well as non-electrical etiologies, and these need to be differentiated since primary electrical dyssynchrony is most likely the only etiology amenable to CRT.

## Cardiac resynchronization therapy

Congestive heart failure is one of the major causes of morbidity and mortality in Norway and other countries. Unlike other common cardiovascular diseases, the age-adjusted mortality attributed to heart failure appears to be increasing. This occurs in spite of several effective drug treatments. Quite recently CRT has been documented to be a powerful treatment in patients with severe congestive heart failure, causing reverse LV remodelling, improvement of symptoms and reduction in mortality (Figure 1) [5, 6].

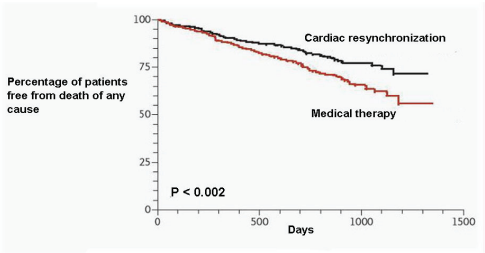


***Figure 1.*** *Right panel: The Care Heart Failure Trial showed marked reduction in mortality with bi-ventricular pacing in severe heart failure (Cleland JG et al, N Engl J Med 2005 14;352:1539-49).*

The principle of CRT is that patients with ventricular dyssynchrony can be resynchronised and improve contractile function through bi-ventricular pacing. This is achieved by using a pacemaker with two ventricular electrodes which activates the right and the left ventricles simultaneously (Figure 2).

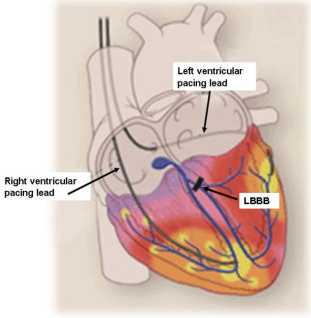


***Figure 2.*** *Schematic illustration of how pacing leads are placed in the two ventricles during bi-ventricular pacing. LBBB = left bundle branch block. Modified from JA Jarcho. N Engl J Med 2006;355:288.*

This technology has evolved rapidly over a few years and is now established as effective treatment in selected patients with congestive heart failure, causing improvement of symptoms, reduction in mortality, and reverse LV remodelling reducing LV volumes. Based on current guidelines, patients selected for CRT must have evidence of intra-ventricular electrical delay with QRS > 120ms, severe congestive heart failure class III or ambulatory class IV, optimal medical therapy, LV ejection fraction ≤ 35 % and evidence of LV dyssynchrony [7]. Recently, guidelines also recommended that patients with heart failure class II and QRS >150ms be considered for CRT [7]. However, based on these guidelines, about one third of patients treated with CRT do not show clinical improvement, and in some cases aggravation of symptoms may occur after implantation of the CRT device [8, 9].

**Therefore, a major problem with CRT is that many patients are non-responders, and we need better methods for selection of candidates for this treatment modality.**

The greatest challenge in the selection of patients for CRT is the verification of dyssynchrony that may respond to resynchronization. Currently, electrocardiography is used as the main screening tool for dyssynchrony, and patients are selected for CRT based on morphology and duration of the QRS complex. In clinical trials which have documented clinical benefit of CRT, one of the entry criteria has been QRS duration over 120 ms and most often with left bundle branch block (LBBB) type morphology and sinus rhythm.

Several trials, however, have shown that QRS duration is not a very precise marker of LV dyssynchrony, as patients with a wide QRS may not have LV dyssynchrony, and patients with a narrow QRS may actually have dyssynchrony. This may explain why a substantial fraction of patients with wide QRS are non-responders to CRT in the large trials [10, 11]. There is therefore a strong interest in developing better methods for identifying patients who will benefit from CRT.

## Assessing regional myocardial function and dyssynchrony

The main methods for assessing regional myocardial function are based on tissue Doppler imaging (TDI) or speckle tracking imaging (STE). These methods allow for analysis of myocardial strain and velocity and have been described and validated in previous studies [12-14]. In short, myocardial strain is a measure of deformation and is defined as fractional change in tissue length expressed as a percentage, and myocardial velocities are measured as rate of myocardial movement relative to a fixed position, usually the apex. A number of echocardiographic indices based on TDI and STE have been introduced and appear to give reliable measures of ventricular mechanical dyssynchrony. The majority of indices use either timing of peak shortening velocity or peak strain (peak shortening) (Figure 3) [15].

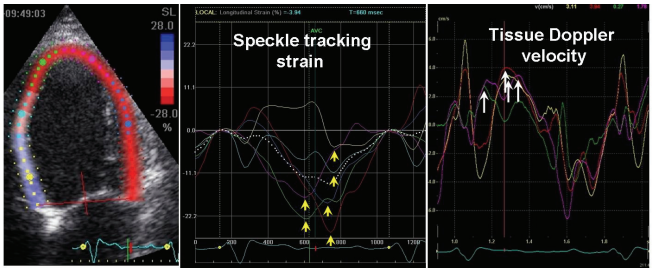


***Figure 3***. *Representative traces from a 4 chamber view in a patient with left bundle branch block. Left panel: traces showing peak strain by speckle tracking echocardiography (yellow arrows). Right panel: traces showing peak ejection velocity (white arrows) by tissue Doppler velocity.*

However, when tested against QRS-width in prospective clinical trials none of the echocardiographic indices have been proven to give clinical benefit in patient selection for CRT [16, 17]. Although QRS duration is an imperfect marker of responders to CRT, there is yet no other consensus definition of dyssynchrony that has been sufficiently evaluated. Therefore, current international guidelines do not recommend routine quantification of dyssynchrony by echocardiography in the evaluation of patients who are considered potential candidates for CRT [7, 18].

One reason for the apparent failure of echocardiography to provide added value in selection of patients for CRT may be that suboptimal methodological approaches have been used. Since it is primarily dyssynchrony caused by electrical conduction delay which will respond to CRT, methodology to differentiate between electrical and non-electrical etiologies of dyssynchrony is important. Furthermore, timing based dyssynchrony indices may not always reflect the hemodynamic consequence of the dyssynchrony, as a dyssynchronous contraction pattern is not only based on the differences in activation between segments but also on differences in regional function i.e. differences in regional work [15, 19, 20].

## Assessing regional myocardial work

In the normal heart all segments contract almost simultaneously. This means that all segments contract against a similar LV pressure. However, when segmental contraction is delayed i.e. one segment contracts after another, this is not the case. In these cases regional contraction within the LV occurs against different pressures and therefore one needs information about both the degree of shortening and LV pressure during shortening to compare regional work done by the segments.

Shortening indices, such as strain, do not incorporate load and do therefore not reflect

myocardial work or oxygen demand. As shown by Suga [21] in an experimental study, the area of the LV pressure-volume loop reflects stroke work as well as myocardial oxygen consumption and the clinical validity of this concept was later confirmed [22]. According to the same principle, the area of the myocardial force-segment length loop reflects regional myocardial work and oxygen consumption [23]. Because calculation of myocardial force is challenging, pressure is used as a substitute for force and the area of the LV pressure-dimension loop is used as an index of regional work [24-27]. The introduction of strain by echocardiography has allowed for non-invasive assessment of regional deformation and may be combined with LVP to assess pressure-strain loops which is likely to provide important insights into cardiac mechanics for assessing myocardial function. However, clinical use of this index is limited by the need for invasive pressure.

## Wasted Work

As discussed above a normal heart will have a synchronous LV contraction of all segments. However, in patients with regional differences in contractility as in ischemia, or delay in electrical conduction as in LBBB, some segments are stretched while others contract, resulting in a dyssycnhronous contraction pattern. The result of this dyssynchrony is that substantial amounts of LV work is "wasted" on stretching opposing segments and does not contribute effectively to LV ejection. Left ventricular electrical dyssynchrony (LBBB) is associated with marked intersegment differences in myocardial work [28]. During LBBB the septum performs little or even negative work, whereas the LV lateral wall is hyperactive due to pre-systolic stretching (increased preload) caused by the early-activated septum. When work is wasted due to electrical dyssynchrony it should in theory, provided the myocardium is viable, be possible to convert the wasted work into effective work if ventricular contractions become resynchronized. Therefore, calculation of wasted work may be an important clinical tool for quantifying the mechanical impact of dyssynchrony on regional and global LV function. Analysis of regional work during electrical dyssynchrony may provide important insights into mechanisms of remodeling and LV dysfunction[29, 30]. Furthermore, abnormal intersegmental work distribution during LBBB is associated with differences in regional blood flow and oxygen demand and may also account for remodeling of the left ventricle [26, 31-33] .

# Aims of the thesis

## General Aims

**The general aim of the present studies was to investigate mechanisms of dyssynchrony and based on this, develop better methods for assessment of patients with dyssynchrony in the heart.**

## Specific Aims

1. The aim of paper 1 was to establish a method which can differentiate between electrical and non-electrical etiologies of left ventricular (LV) dyssynchrony, because primary electrical dyssynchrony is most likely the only etiology amenable to CRT.

2. During left bundle branch block (LBBB) electromechanical delay (EMD), defined as time from regional electrical activation (REA) to onset shortening, is prolonged in the late activated left ventricular (LV) lateral wall compared to the septum. The aim of paper 2 was to determine the mechanism of the prolonged EMD allowing for a better understanding of dyssynchrony measurements that rely on timing of regional myocardial shortening.

3. The main objective of paper 3 was to determine if LV pressure-strain loop area can be estimated with an entirely non-invasive approach by using an estimated LV pressure curve in combination with strain by speckle tracking echocardiography. Furthermore, to investigate if non-invasive pressure-strain area reflects regional work and metabolism.

4. The main aim of paper 4 was to investigate if LV work that is wasted during dyssynchronous LV contraction can be measured and quantified non-invasively using wasted work fraction (WWF).

# Materials

## Experimental studies

**In vivo study (Papers 1-4)**

A total of 15 mongrel dogs were studied. In 7 dogs LBBB was induced by radiofrequency ablation [34] and in 8 dogs ischemia was induced by occlusion of the left anterior descending coronary artery.

**In vitro study (Paper 2)**

Four New Zealand White rabbits were used for the papillary muscle study.

The National Animal Experimentation Board approved the study. The laboratory animals were supplied by Center for Comparative Medicine, Oslo University Hospital, Rikshospitalet, Norway.

## Clinical studies

**Electromechanical delay group (Paper 2)**

Nine patients with heart failure (NYHA II-IV) and implanted bi-ventricular pacing devices were included (3 patients with ischemic cardiomyopathy and 6 patients with non-ischemic dilated cardiomyopathy). All patients had LBBB before implantation of the CRT pacing device.

**Invasive LV pressure group (Paper 3 and 4)**

Eighteen patients with heart failure (NYHA II-IV) underwent LV catheterization, including 11 with ischemic cardiomyopathy and 7 with non-ischemic dilated cardiomyopathy. Twelve of these patients had LBBB. Four of the patients with LBBB had a CRT device allowing for echocardiographic measurements with CRT on and off with color tissue Doppler imaging (Paper 2), however, only two had image quality sufficient for STE (Paper 3).

**Positron Emission Tomography group (Paper 3)**

Six patients with dilated cardiomyopathy and LBBB (NYHA II-IV) were included for $^{18}$F-fluorodeoxyglucose positron (FDG-PET) analysis. In these patients coronary artery disease was ruled out by coronary angiography prior to investigation.

**Cardiac Resynchronization Therapy Group (Paper 4)**

Ten patients with heart failure (NYHA II-IV) and LBBB were included. In these patients coronary artery disease was ruled out by coronary angiography prior to investigation. Echocardiography was preformed prior to CRT implantation and at follow up 8±3 months after implantation.

**Control group (Paper 4)**

Twenty healthy individuals were age and sex matched and recruited from hospital staff. All had normal clinical examination, ECG and echocardiography.

All studies were approved by the Regional Committee for Medical Research Ethics and all subjects gave written informed consent.

# Models and Methods

## Experimental studies

**In vivo animal model (Papers 1-4)**

**Animal preparation**

The dogs were anesthetized, ventilated, and surgically prepared as previously described [35]. In addition pacemaker leads were attached epicardially on the left ventricular lateral wall and right atrium and endocardially in the right ventricular outflow tract close to the septum. Aortic, left atrial and LV pressures were measured by micromanometers [35]. A fluid-filled catheter in the left atrium served as an absolute pressure reference.

**Sonomicrometry and regional electromyograms**

In each dog 2 mm sonomicrometry crystals (Sonometrics Corp., London, Ontario, Canada) with bipolar electrodes for measuring IM-EMG were implanted sub-endocardially and sub-epicardially as illustrated in Figure 4. In each of the dogs 4 circumferential and 2 longitudinal (anterior and posterior) segments were measured. In the animals with LBBB we additionally measured longitudinal dimension in the mid-segments in septum and lateral wall.

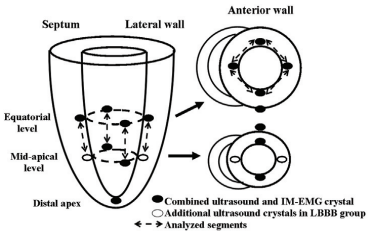


***Figure 4**. Schematic illustration of placement of myocardial crystals.*[36]

Depending on the specific aim of the study, various combinations of crystal pairs were analyzed and reported (as described in the papers). Timing of regional electrical activation was measured at onset R in IM-EMG, defined as the onset of the first spike that lead to a deflection of more than 20% of total QRS amplitude.

**Echocardiography**

A Vivid 7 ultrasound scanner (GE Vingmed Ultrasound AS, Horten, Norway) was used to record color-coded TDI images in apical 2, 4 and long chamber views. Conventional 2-D grayscale images of the LV equatorial short-axis and apical long axis, 2 and 4 chamber views were acquired for STE.

## Data analysis - Experimental studies

**Regional strain and shortening velocity (Paper 1)**

Myocardial strain was obtained by sonomicrometry calculated as a percentage of end-diastolic length, and strain by echocardiography using STE. Myocardial shortening velocity by sonomicrometry was calculated as the time derivative of segment length and shortening velocity by echocardiography using TDI. The following time markers were measured for myocardial shortening velocity and strain:

- Timing of onset of systolic shortening velocity

- Timing of peak shortening velocity during ejection (S)

- Timing of peak systolic strain.

**Onset active force generation (AFG) by sonomicrometry and LVP (Paper 1 and 2)**

The time of onset AFG was determined by analyzing myocardial pressure-segment length loops, and was defined as the time when the pressure-segment length coordinate was shifted upwards relative to the passive-elastic curve for the same segment. The calculation of onset AFG is illustrated in Figure 5. The passive-elastic curve was constructed by an exponential fit to a series of end-diastolic pressure-segment length coordinates obtained during caval constriction (Figure 5, left panel i-iii). End-diastolic measurements were used in order to ensure that the myocardium was completely relaxed. Onset AFG was defined as the time when the pressure-segment length coordinate was shifted upwards relative to the passive-elastic curve for the same segment (Figure 5, middle panel). Since the pressure-segment length relationship provides no timing information, onset AFG was extracted from a corresponding time point in either the pressure or the segment length curve (Figure 5, right panel).

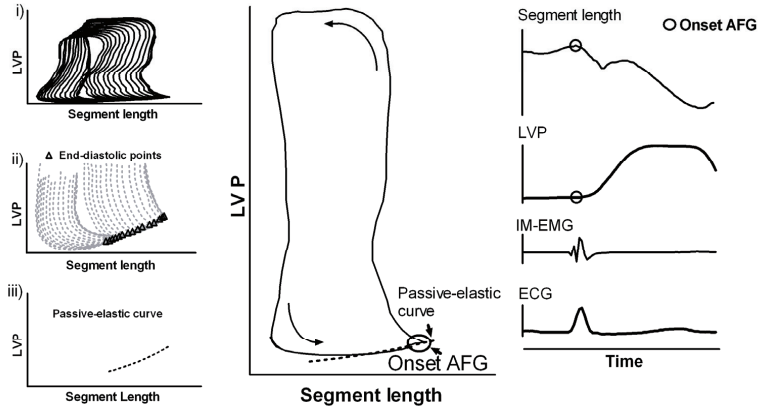


***Figure 5****. Measurement of onset active force generation (AFG) in a representative experiment.* ***Left panel.*** *Construction of passive elastic curve. i) Pressure-segment length loops during caval constriction. ii) High gain LV pressure (LVP) showing end-diastolic points. iii) Exponential fit to end-diastolic points.* ***Middle panel.*** *Onset AFG was defined as the first coordinate of the pressure segment length loop that leads to a deviation from the passive-elastic curve.* ***Right panel****. Timing of onset AFG was extracted from either LVP or segment length traces.*[36]

**Onset AFG by STE and LVP (Paper 1)**

Onset AFG was also assessed by combining LVP with strain by STE. Because strain represents a relative value, this analysis does not provide a range of end-diastolic pressure-dimension relations, and the late-diastolic portion of each loop was used to define the passive-elastic state. Identification of onset AFG was based on subjective, visual assessment, defined as the first marked upward deviation of the pressure-strain loop that resulted in a continued upward shift after onset of R in ECG.

**Quantification of LV dyssynchrony (Paper 1):**

Left ventricular dyssynchrony was quantified by two different approaches; 1) as peak intersegment time difference, measured as time difference between the earliest and the latest activated segments, and 2) as standard deviation for 6-8 segments of time from onset R in ECG to timing of each of the indices, referred to as *SD of timing*. In addition we presented times from onset R in ECG to timing of each of the indices. The latter approach allows presentation of individual timing data from all segments and all animals in a single graph.

**Electromechanical activation time (Papers 1 and 2)**

*Electromechanical delay* (EMD) for LV septal and lateral wall segments was quantified by two different approaches: 1) as time from regional electrical activation to onset of shortening ($EMD_{OS}$), and 2) as time from regional electrical activation to onset of active force generation ($EMD_{AFG}$). Timing of onset AFG (as defined above) reflects the earliest mechanical sign of active force and we therefore used $EMD_{AFG}$ as the reference method for electromechanical coupling time.

**Calculation of estimated LV pressure curve (Paper 3 and 4)**

The non-invasively estimated LV pressure curve was validated first in the dog model which allowed testing under a wide range of hemodynamic conditions. Thereafter, the method was validated in patients with various cardiac disorders. As an estimate of peak LV pressure, aortic pressure measured invasively was used in dogs and brachial artery cuff pressure in patients. The profile of the estimated LV pressure curve was determined by using an empiric reference curve which was adjusted according to duration of the isovolumic and ejection phases as determined by echocardiography.

*Calculating LV pressure reference curve*

The LV pressure reference curve was calculated by pooling single cycle LV pressure traces from all interventions and normalizing each pressure trace using timing of valvular events in the following three steps: 1. The timing of opening and closure of the mitral and aortic valves was identified by echocardiography and assigned to each of the pressure traces (Figure 6 A1 and B1). 2. Each of the raw data traces were stretched or compressed along the time axis between individual valve events in order to make the valvular events coincide for all recordings (Figure 6 A2 and B2). 3. All traces were scaled vertically to have the same peak value. An averaged waveform was then calculated (black line in black Figure 6 A2 and B2).

*Applying LV pressure reference curve to a specific subject*

The profile of the averaged LV pressure waveform was used for predicting LVP in the specific subject by measuring the actual valvular timing for the relevant cardiac cycle and adjusting the duration of time intervals of IVC, ejection and IVR phases by stretching or compressing the time axis of the averaged LV pressure curve to match the measured time intervals (Figure 6 B3 and 4). Peak arterial pressure was used to scale the amplitude of the pressure curve. Separate reference curves were used for dogs and patients. Note that data from all interventions in the dog study were used and that data from all patient observations were included in the

calculation of the normalized LV pressure reference curve without considering their clinical status.

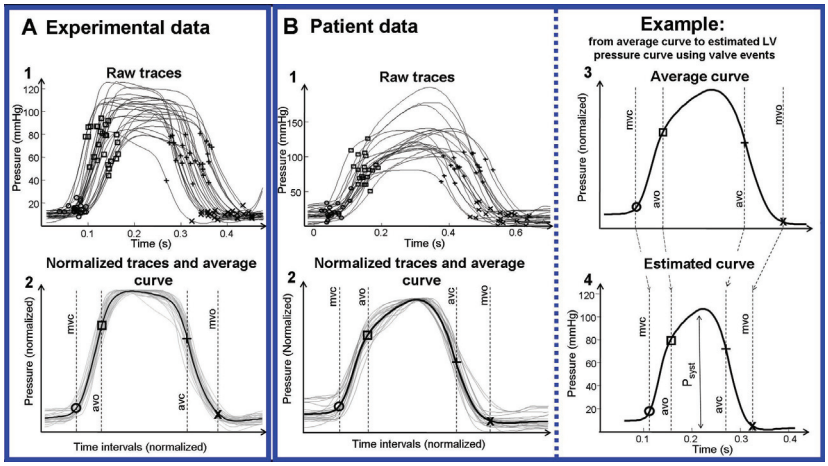


***Figure 6.*** *Estimation of LV pressure curve* ***A. 1)*** *Raw LV pressure data from dogs used for creating a profile of the reference pressure waveform, consisting of pressure recordings during different haemodynamic situations. Timing of mitral and aortic valve events are indicated.* ***2)*** *The raw pressure waveforms (grey curves) have been stretched or compressed along the time axis between individual valve events in order to make the valvular events coincide for all recordings. The waveforms have also been vertically scaled to have the same peak value. The averaged waveform to be used for predicting pressure traces is indicated by the black curve.* ***B. 1 and 2)*** *Patient data: estimation of average pressure waveform as described in A.1 and 2.* ***3)*** *The averaged waveform with arbitrary time intervals, transferred from panel B.2.* ***4)*** *Prediction of the LV pressure waveform is based on timing of valvular event. The LV pressure waveform is constructed by adjusting the duration of time intervals to match the actual valvular timing as determined by echocardiography in the specific subject. In addition to the time axis adjustments, the waveform has been scaled according to systolic arterial cuff pressure* [37].

**Pressure strain loops (Paper 3)**

Strain and pressure data were synchronized using onset R in ECG as a common time reference. Strain by STE was converted to the same sampling rate as sonomicrometry (200 Hz). Loop area was calculated by the following methods:

1.*Invasive method:* The area of the LV pressure-strain loops by LVP and STE.

2.*Non-invasive method*: The area of the LV pressure-strain loops by the estimated LV pressure curve and STE.

**Comparison between LV pressure-strain loop area and myocardial work**

LV pressure-strain loop area as an index and myocardial work does not take into account effects on work related to changes in radius of curvature or contribution from different fibre directions. To determine the magnitude of this effect we measured myocardial work incorporating LV geometry (circumferential and longitudinal) and area strain during LBBB. To be able to compare the two methods we correlated work done by the septum divided by work done by the lateral wall using the two methods. A comparison between septum and lateral wall was made because during LBBB the septum does less work compared to the lateral wall.

**Calculation of segmental work as a function of time**

Work for individual segments as a function of time throughout the cardiac cycle was calculated from the strain recordings and from measured or estimated LV pressure. This was done by obtaining the rate of segmental shortening (strain rate) by differentiation of the strain curve (Figure 7 A), and multiplying this with instantaneous left ventricular pressure (Figure 7 B). This resulted in a measure of instantaneous power, which was integrated over time to give work as a function of time (Figure 7 C). Performing this calculation for the IVC, ejection and IVR phases of a cardiac cycle is mathematically the same as calculation of the area between the x-axis and the corresponding segment of the strain – pressure loop, however keeping in mind that areas under sections of the loop that represent elongation are counted as negative.

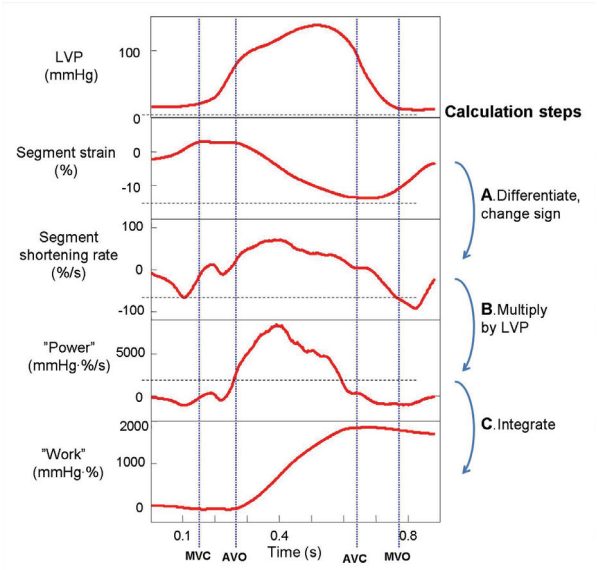


***Figure 7.*** *Work of individual segments was calculated from the strain recordings and the left ventricular pressure. Instead of calculating only one value of work in a completed cardiac cycle for each segment, equal to the area of the strain – pressure loop, work was calculated as a function of time throughout the cardiac cycle. This was done by obtaining the rate of segmental shortening (strain rate) by differentiation of the strain curve (Figure 7A), and multiplying this by instantaneous left ventricular pressure (Figure 7B). This resulted in a measure of instantaneous power, which was integrated over time to give work as a function of time (Figure 7C) (From Paper 4).*

**Analysis of segment work curves**

Information was extracted from the segmental work curves over a time interval spanning from mitral valve closure to mitral valve opening. The following variables were calculated:

$W_{pos}$ Total positive work, sum of all work performed during shortening of the segment (Figure 8, red line).

$W_{neg}$ Total negative work, sum of all work performed during elongation of the segment (Figure 8, black line).

WWF was calculated globally from the sum of work for all segments:

$$WWF_{global} = 100 \cdot \frac{\sum W_{neg}}{\sum W_{pos}}$$

The net work contributing to systolic ejection for each segment was calculated as:

$$W_{net} = W_{pos} - W_{neg}$$

A segmental Negative/Positive work ratio for each segment was also calculated:

$$Segmental\ negative\ /\ positive\ work\ ratio = \frac{W_{neg}}{W_{pos}}$$

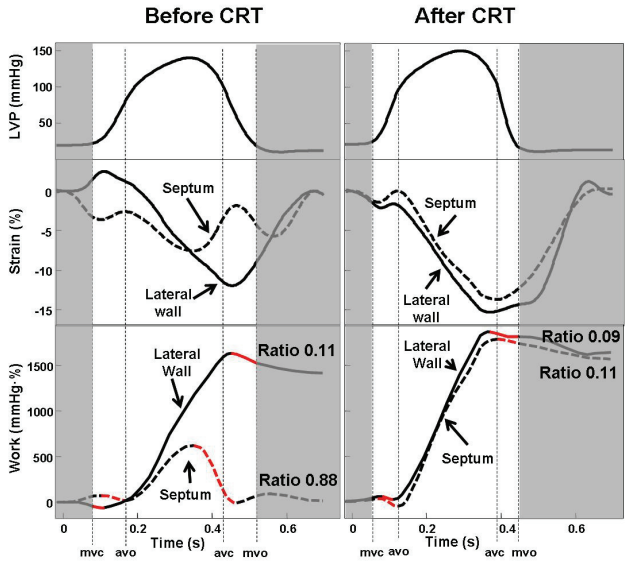


**Figure 8.** Estimated LV pressure (upper panels), strain (middle panels) and calculation of wasted work for septum and lateral wall (lower panels) in a representative patient with left bundle branch block (LBBB) (left panel) and after treatment with cardiac resynchronization therapy (CRT) (right panel). Horizontal lines indicate valvular events measured by echocardiography. In the lower panels negative and positive work during systole is marked as red and black, respectively. In lower panels the segmental Negative/Positive work ratios are indicated. Please note that the ratio improved markedly in the septum with CRT, indicating a conversion to predominantly positive work. (From paper 4)

## In vitro Papillary Muscle Study (Paper 2)

**Quantification of Electromechanical Delay**

The papillary muscles were extracted and prepared as described in paper 2.

Onset of electrical activation was defined as the start of the stimulation spike. Onset of shortening was defined as the first data point after peak length of the papillary muscle that led to continued shortening.

To assess if the load at the time of activation affected the delay from electrical activation to OS, we activated the papillary muscle at different isotonic loads: F= 40, 50, 60, and 70% of Fmax (Figure 9 A) where Fmax was peak isometric force developed by the muscle. We subsequently measured time from electrical activation to OS.

To assess if rate of load rise (dF/dt) at time of activation (equivalent to dP/dt in the in vivo heart) affected the delay from electrical activation to OS, we activated the papillary muscle and applied linearly increasing load (dF/dt) at different slopes from the time of electrical activation (Figure 9 B), i.e. ramp loading. Different slopes were applied by linearly increasing F from preload to 40, 50, 60, and 70% of Fmax in a constant time interval. (Figure 9 B).

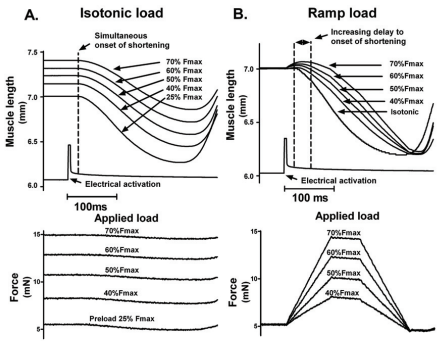


***Figure 9.*** *Papillary muscle experiment.* ***A.*** *Delay in onset shortening as a function of isotonic load* ***B.*** *Delay as a function of dF/dt* [38].

# Clinical studies

**Echocardiographic and Hemodynamic measurements (Papers 2-4)**

For all patients a Vivid 7 ultrasound scanner (GE) was used to record color-coded TDI images in apical 2, 4 and long chamber views. Conventional 2-D grayscale images of the LV equatorial short-axis and apical 2, 4 and long chamber views were acquired for speckle tracking echocardiography (STE). In the six patients who underwent PET echocardiography was performed immediately after the PET.

In the 18 patients with invasive measurements, LVP was measured by a micromanometer-tipped catheter (Millar Mikro-Tip SPC-454F, Houston, Texas) and a fluid-filled catheter connected to an external pressure transducer served as absolute pressure reference. Brachial arm cuff pressure was measured. Pressure and imaging data were stored on the ultrasound scanner. All the analysis was performed offline.

**Assessing electro mechanical activation (Paper 2)**

Regional electrical activation for septum and lateral wall was assessed using the pacemaker electrodes as regional EMGs. Onset of regional electrical activation was defined as onset R in EMG as described above. Onset of shortening was assessed in septal and lateral wall segments corresponding to lead position using longitudinal strain by TDI. Time from regional electrical activation to OS ($EMD_{OS}$) for the septum and lateral wall was then calculated for each patient with pacing ON and OFF. In four patients LVP was measured by micromanometry and simultaneous echocardiographic recordings were performed.

**FDG-PET (Paper 3)**

Patient preparation is described in paper 3 and in previous publications [39]. Gated FDG-PET acquisition (Simens Biograph 64) was started 60-80 min after intravenous administration of the FDG (370-380 MBq ), with 8 gates per RR interval. The acquisition was also gated for respiration. Images were reconstructed and analyzed on the Xeleris workstation (GE healthcare). The point in the LV myocardium with the highest FDG uptake was used as a reference (100%), and segmental values were reported as percentages of this value.

## Data analysis - Clinical studies

### Pressure-strain loops (Paper 3)

The non-invasively estimated LV pressure curve was constructed using the same approach as described in the experimental study section. As an estimate of peak LV pressure, brachial artery cuff pressure was measured in patients. The profile of the estimated LV pressure curve was determined by using an empiric reference curve which was adjusted according to duration of the isovolumic and ejection phases as determined by echocardiography (Figure 6 B and C). Separate reference curves were used for dogs and patients (Figure 6 A and B). Note that data from all interventions from all patient observations were included in the calculation of the normalized LV pressure reference curve without considering their clinical status.

### Wasted work fraction

*Echocardiography and estimated vs. invasive LV pressure*

In the patients with invasive LV pressure, work was analyzed by two different methods: 1. STE strain and measured LV pressure 2. STE strain and estimated LV pressure.

*Echocardiography and estimated LV pressure*

To assess responses to CRT, work analysis was performed before implantation of the CRT device and at 8±3 months follow up, using estimated LV pressure and strain from the 3 apical views. Measurements were also performed in the normal control population using the same approach.

### Statistical analysis

Values are expressed as mean±SD. Variables were compared using least-squares linear regression, Pearson correlation coefficients, intraclass correlation coefficients and Bland-Altman methods. To account for multiple measurements from each animal when using Bland-Altman we display reference intervals based on agreement between methods of measurement with multiple observations per individual [40]. Significance for mean difference was assessed using paired t-test method. For multiple comparisons we used two-way repeated measurements ANOVA with LSD post test (SPSS 15.0, SPSS Inc, Chicago, IL). All post hoc tests are compared to baseline. $P<0.05$ was considered significant.
Interobserver variability was assessed using the interclass correlation coefficient (α value) and Bland-Altman method.

# Summary of results

## Paper 1.

In fourteen anesthetized dogs we induced ischemia by occluding the left anterior descending artery (n=8) and bundle branch block (LBBB) by radiofrequency ablation (n=6). LV *mechanical* dyssynchrony was evaluated by two different approaches. First, we measured timing of peak myocardial shortening velocity and strain. Secondly, we measured first sign of tension development by onset AFG as defined by myocardial pressure-segment length loops upward shift from its passive-elastic state (Figure 5). *Electrical* dyssynchrony was measured by intramyocardial electromyograms (IM-EMG). Dyssynchrony was quantified as peak intersegment time difference and as standard deviation of timing for 6-8 myocardial segments.

During baseline, reduced preload and myocardial ischemia shortening velocity and strain indicated segmental mechanical heterogeneity, while onset AFG and onset R in IM-EMG indicated synchronous activation of all segments (Figure 10). After induction of LBBB all methods indicated dyssynchrony. Peak intersegment time difference for shortening velocity and strain showed moderate correlations (r=0.57 and 0.32) and weak agreements (mean differences, -47±27 and -28±27 ms, respectively) with IM-EMG. Onset AFG by pressure-segment length loops, however, correlated well with IM-EMG (r=0.93), and agreement was good (mean difference, -0.6±6.8 ms). Results were similar for standard deviation of timing. Onset AFG from pressure-strain analysis by echocardiography showed accuracy similar to sonomicrometry.

Onset AFG was an accurate marker of myocardial electrical activation, and was superior to shortening velocity and strain. Identification of electrical dyssynchrony by onset AFG may be feasible clinically using LV pressure-strain analysis.

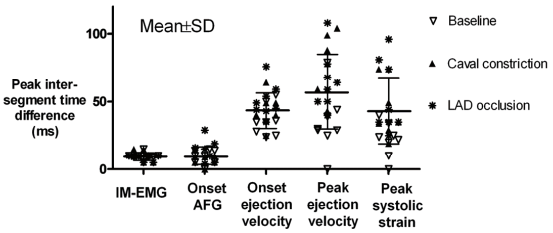


***Figure 10.*** *Peak intersegment time difference during baseline, load alteration and ischemia illustrating the variability in different dyssynchrony indices. Lines show mean±SD* [36].

## Paper 2.

In an experimental LBBB dog model (n=7), in patients (n=9) with bi-ventricular pacing devices, in an in vitro papillary muscle study (n=6), and a mathematical simulation model we measured left ventricular pressures, myocardial deformation, and regional electrical activation (REA). In the dogs, there was a greater mechanical than electrical delay (82±12 vs. 54±8 ms, $p$=0.002) due to prolonged EMD in the lateral wall vs. septum (39±8 vs.11±9 ms, $p$=0.002). The prolonged EMD in later activated myocardium could not be explained by increased excitation-contraction coupling time or increased pressure at the time of REA, but was strongly related to dP/dt at the time of REA (r=0.88, Figure 11 A). Results in humans were consistent with experimental findings. The papillary muscle study showed that EMD was prolonged at higher dF/dt because it took longer for the muscle to generate active force at a rate superior to the load rise which is a requirement for shortening (Figure 11 B) and these findings were also supported by a mathematical model.

We conclude that during LBBB prolonged EMD in late activated myocardium is caused by a higher dP/dt at the time of activation, resulting in aggravated mechanical relative to electrical dyssynchrony. These findings suggest that LV contractility may modify mechanical dyssynchrony.

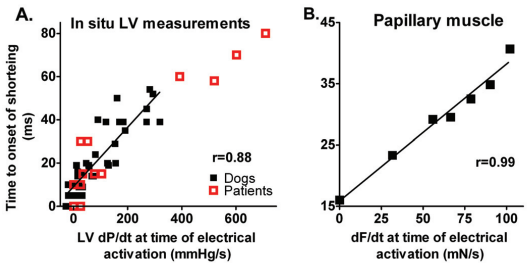


***Figure 11. A.*** *Correlation for pooled data between dP/dt and time from regional electrical activation to onset of shortening. R value for animal data only.* ***B.*** *Correlation between dF/dt and time from electrical activation to onset of shortening for a representative papillary muscle* [38].

## Paper 3.

In an experimental dog model (n=12) and in patients (n=18) pressure-strain loop area was measured using measured left ventricular pressure (LVP) and estimated LVP. LVP was estimated by utilizing the profile of an empiric, normalized reference curve which was adjusted according to duration of LV isovolumic and ejection phase, as defined by timing of

aortic and mitral valve events by echocardiography. Absolute LV systolic pressure was set equal to arterial pressure measured invasively in dogs and non-invasively in patients. In 6 patients myocardial glucose metabolism was measured by positron emission tomography (PET). First, we studied anaesthetized dogs and observed strong correlation (r=0.96) and good agreement between estimated LV pressure-strain loop area and loop area by LV micromanometer and sonomicrometry. Secondly, we validated the method in patients with various cardiac disorders, including LV dyssynchrony and confirmed strong correlation (r=0.99) and good agreement between pressure-strain loop areas using non-invasive and invasive LV pressure. Non-invasive pressure-strain loop area reflected work calculated using changes in LV geometry and 2-D strain (r=0.97), and showed good correlation with regional myocardial glucose metabolism by PET (r=0.81) (Figure 12).

The novel non-invasive method for regional LV pressure-strain loop area corresponded well with invasive measurements and with directly measured myocardial work and it reflected myocardial metabolism. This method for assessment of regional work may be of clinical interest for several patient groups, including LV dyssynchrony and ischaemia.

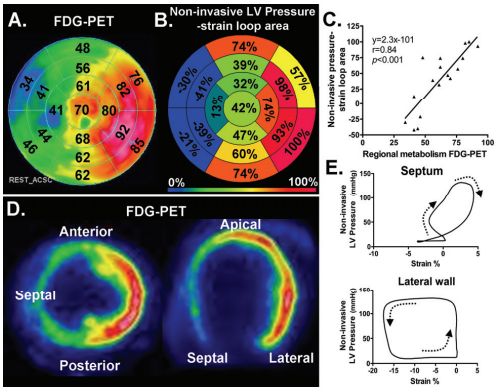


***Figure 12.*** *Data from one representative patient* ***A)*** *Bull's-eye plot showing relative glucose metabolism by FDG-PET in a representative patient with LBBB. The point in the LV myocardium with the highest FDG uptake was used as a reference (100%), and segmental values were reported as percentages of this value.* ***B)*** *Bull's-eye plot with similar anatomical distribution as in A. showing relative loop area by estimated LV pressure and STE. The segment with the largest loop area was used as a reference (100%), and segmental values were reported as percentages of this value.* ***C)*** *Correlation between regional metabolism by FDG-PET and loop area by estimated LV pressure and STE.* ***D)*** *Representative pictures showing regional distribution of glucose metabolism by FDG-PET for short axis (left panel)*

*and four chamber (right panel) views.* ***E)*** *Estimated LV pressure and STE loops from septum and lateral wall* [37].

## Paper 4.

Segmental work was calculated by multiplying strain rate by LV pressure (LVP) to get instantaneous power, which was integrated to give work as a function of time (Figure 7). The WWF was calculated as work consumed during segmental lengthening (wasted work) as a fraction of work during segmental shortening. A non-invasive LVP curve was derived using the previously validated method described in paper 3, and was combined with strain by speckle tracking echocardiography (STE) to calculate WWF non-invasively. The non-invasive WWF was validated in 6 anesthetized dogs against WWF by invasive LVP and sonomirometry, and in 18 patients against invasive LVP and strain by STE. Effect on WWF by cardiac resynchronization therapy (CRT) was studied in 10 patients with left bundle branch block (LBBB).

The validity of non-invasive WWF was confirmed in the dog model by strong correlation (r =0.94) and good agreement with WWF by micromanometer and sonomicrometry. Furthermore, in patients, non-invasive WWF showed strong correlation (r =0.96) and good agreement with WWF using invasive LVP (Figure 13). Finally, we showed that WWF during LBBB was reduced from 36±16 to 17±7%, ($p<0.001$) in CRT responders.
WWF quantifies "wasted work" that may contribute to global LV function if synchronized, and may serve as an important tool when evaluating the effect of CRT and optimizing device settings.

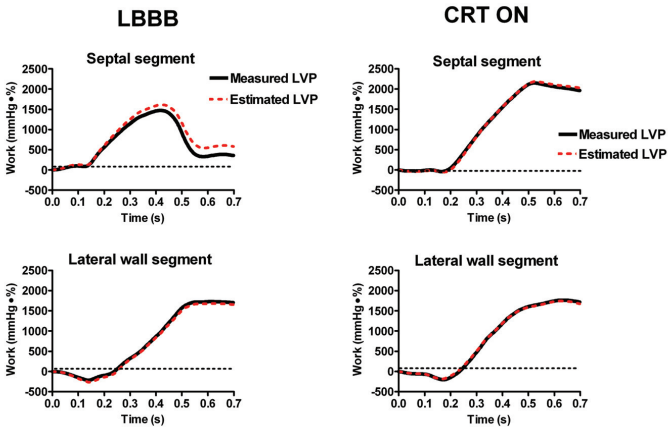


***Figure 13.*** *Work analysis by LVP and speckle tracking echocardiography (STE) (solid line) vs. the non-invasive method by estimated LVP and STE (dashed line), for a septal and lateral wall segment in patient with the CRT device turned on and off. (From paper 4)*

# Discussion

## Differentiation between electrical and non-electrical dyssynchrony.

In a clinical setting the differentiation between dyssynchrony with electrical and non-electrical etiologies is essential since electrical dyssycnhrony is most likely the one etiology amenable to CRT. Paper 1 introduces assessment of onset of active force generation as a method to quantify LV electrical dyssynchrony and to differentiate between electrical and non-electrical dyssynchrony. Unlike the QRS duration, onset AFG gives regional information and allows for direct comparison between LV walls. The principle behind this novel method is that onset of active force generation is the first mechanical sign of actine-myosin interaction, and in contrast to indices based only on myocardial velocity and strain, it is independent of loading conditions and contractility.

When using pressure-dimension curves, active forces are verified by showing an upward-shift of the LV pressure-segment length relation relative to the passive-elastic curve. An upward-shift means that a higher pressure (or force) is needed to distend the segment to a given length, which implies that stiffness is increased. With this approach onset AFG can identify mechanical activation even in segments with systolic lengthening.

During changes in load, myocardial ischemia and LBBB, the electro-mechanical activation time was essentially constant, hence, onset AFG tracked changes in timing of electrical activation. Accordingly, onset AFG, which primarily is a measure of mechanical activation, was an accurate measure of electrical activation as well. The AFG method was feasible not only with sonomicrometry, but also when strain by STE was used as an analog for segment length, suggesting a potential for measuring onset AFG clinically during left heart catheterization. Using onset R in IM-EMG as reference method for electrical dyssynchrony, we demonstrated that onset AFG was superior to conventional timing indices based on myocardial velocity and deformation.

Consistent with the study of Ruffy et al [41] we observed no significant delay in subendocardial electrical activation during short term ischemia. Therefore, electrical delay could not account for the observed dyssynchrony during ischemia. Possibly, more severe and longer lasting ischemia could induce conduction delays. The aim of paper 1, however, was to determine if onset AFG could identify mechanical activation in segments with decreased regional contraction and we therefore used ischemia to depress myocardial function. Furthermore, the principle of onset AFG is such that it should identify delay in electrical activation regardless of etiology.

## Electro-mechanical delay during left bundle branch block

The finding in paper 1 that electromechanical delay remained unchanged after induction of LBBB is in apparent contrast to previous studies which have used epicardial sensors to measure electromechanical delay. Prinzen et al showed increased electromechanical delay (time from electrical activation to onset shortening, $EMD_{OS}$) in the latest activated segments during pacing in the right ventricular outflow tract [42]. However, the different findings in our study can be explained by the different definition of mechanical activation: i.e. onset AFG vs onset of shortening. In paper 2 we investigated the mechanism of the apparently prolonged electromechanical activation time in late activated LV lateral wall during LBBB. As described in paper 1 we did not observe any indication of prolonged excitation-contraction coupling time (time form electrical activation to onset AFG, $EMD_{AFG}$) in the late activated region. Furthermore, increased load (LVP) at time of electrical activation in the late activated lateral wall showed a weak relationship to the increased $EMD_{OS}$, and was not significant when adjusted for the increased dP/dt at time of activation. However, there was a strong correlation between dP/dt at time of activation and delay in OS. The findings from the different sub-studies indicate that OS is delayed until rate of rise in myocardial active force exceeds rate of rise of applied load. Since rate of rise of regional load in the intact heart is directly related to LV dP/dt, there will be a progressive increase in time from electrical activation to OS at higher LV dP/dt.

Our results suggest that the prolonged delay from electrical activation to OS in late activated segments increases the mechanical dyssynchrony by ~40-50% relative to the underlying electrical dyssynchrony, e.g. electrical dyssynchrony of 54 ms vs. mechanical dyssynchrony of 82 ms in the dog model. In a clinical setting understanding the mechanism of the prolonged delay is important for two main reasons: 1. Onset of shortening may potentially influence almost all dyssynchrony measurements performed by echocardiography. Because time from electrical activation to OS differs substantially between early and late activated segments this means that OS may not serve as an accurate marker for electrical activation in assessment of dyssynchrony. 2. Mechanical dyssynchrony measured as differences in OS, is dependent on both electrical propagation time in the LV and differences in regional $EMD_{OS}$. This means that prolongation of $EMD_{OS}$ in late activated segments may aggravate mechanical dyssynchrony, subsequently reducing LV function. Furthermore, since LV dP/dt reflects LV function and contractility, the magnitude of mechanical dyssynchrony may vary over time in a given patient when there are changes in LV function.

Intuitively one may believe that it is the higher pressure at time of activation of the lateral wall that is responsible for the increased delay from regional electrical activation to OS. However, in the dog study in paper 2 we found that it was not LVP at time of regional

activation, but rate of pressure rise (LV dP/dt) that directly affected the delay from electrical activation to OS. To further investigate this we performed a papillary muscle study where these two mechanisms could be isolated and tested in a controlled environment. When a constant force was applied, OS occurred without increased delay even when applied force was substantially increased (70% of Fmax) (Figure 9 A). However, when we applied a rising force (simulating continuous rise in LVP), time to OS was progressively delayed with higher dF/dt (Figure 9 B).

Segmental force is a sum of both active and passive elastic forces which is equal to the external load according to Newton's 3rd law. Prior to activation a higher pressure stretches and hence increases the passive force of a late activated segment, thus maintaining the balance of external and internal forces. Subsequent activation and addition of active force should therefore result in instantaneous OS of the segment. However, a late activated segment does not contract against a static pressure, but a pressure that has already started to rise. The pressure rise continues to stretch the segment until the generation of opposing contractile force is faster than the load rise. Active force development is nonlinear, i.e. it initially increases at a slow rate and gradually accelerates to peak rate [43]. Therefore, the higher the LV dP/dt, the longer it takes before active force is generated at a rate equal to and subsequently faster than load rise, which delays OS and prolongs $EMD_{OS}$.

In summary papers 1 and 2 introduce assessment of onset of active force generation as a method to quantify LV electrical dyssynchrony and to differentiate between electrical and non-electrical dyssynchrony. Furthermore, they show that electro-mechanical activation time was essentially constant during changes in load, myocardial ischemia and LBBB, however, time from regional electrical activation to onset of shortening depended on rate of LV pressure rise at time of activation suggesting that timing of onset shortening may be affected by LV contractility.

## A non-invasive index of myocardial work

In paper 3 we demonstrate that LV pressure-strain loop area, which is an index of regional LV work, can be measured clinically by an entirely non-invasive approach. This was feasible by combining a non-invasive LV pressure analog with strain by STE. The validity of this method was confirmed in the experimental part of the study by an excellent correlation and good agreement with loop area by pressure-segment length analysis. In the clinical study LV pressure-strain loop area using the non-invasive LV pressure analog showed strong correlation and good agreement with loop area using invasive LV pressure. When the non-invasive pressure-strain assessment was applied in patients with LBBB we observed marked

non-uniformity in regional work distribution with reduced work in the septum and increased work in the LV lateral wall, suggesting that the work analysis may represent a means to explore the hemodynamic impact of electrical dyssynchrony and to monitor responses to CRT. Non-uniformity in work distribution was also apparent when comparing ischemic vs. non-ischemic segments. Furthermore, we show that this non-invasive method reflects both regional metabolism and work calculations incorporating changes in LV geometry which strongly supports its use as a regional work index.

**Calculation of work**

In principle, the area of the myocardial force-dimension loop represents regional LV work and may also be used as a mechanical index of regional myocardial oxygen consumption [23]. In the present study we used pressure as a substitute for force and the area of the LV pressure-strain loop was used as an index of regional work. This index does not provide a measure which has units of work, and does not incorporate the modifying effect of local radii of curvature or contributions from different fiber orientations on force. To address these issues and in particular to explore how changes in septal curvature during LBBB would modify the ability of septal pressure-strain loop area to reflect the force-strain loop area, we performed additional analysis. There was a good correlation between relative work using the two methods (r=0.97), indicating that the pressure-strain loop area gives adequate clinical information regarding relative differences in work distribution within the same heart. Furthermore, in our laboratory we have previously demonstrated that changes in segmental pressure-dimension loops approximate changes in the stress-dimension loops during myocardial ischemia [44].

The ability of pressure length area to reflect myocardial oxygen consumption has been shown previously [26]. In the present study we found that the non-invasive LV pressure-strain loop area had good correlation and agreement with regional glucose metabolism using FDG-PET. Previous studies have shown that glucose metabolism reflects myocardial work [45], and this finding therefore supports our conclusion that pressure-strain loop area reflects differences in myocardial work distribution. The present findings of regional changes in work distribution in patients with LBBB are in keeping with the observations by Prinzen et al [46] in a dog model with right ventricular pacing.

**Estimated LV pressure curve**

There are numerous techniques which can provide a more accurate central aortic pressure than just using brachial artery cuff pressure, and these may be applied in combination with the present method. However, when the non-invasive pressure method is used for comparing work between segments, the main issue is the abnormal distribution of work and not the absolute values.

It is important to note that the only application of the non-invasive pressure curve proposed in this study was to serve as a pressure estimate when calculating LV pressure-strain loop areas, and for this application it served its purpose very well, as indicated by the excellent relationship to reference methods for pressure-loop area. It does not have sufficient accuracy, however, to provide a measure of LV diastolic pressure or peak rate of rise or fall in LV pressure.

Whereas correct timing of peak LV pressure was of little importance for pressure-strain loop area, errors in timing of early systolic rise in pressure (IVC) and early-diastolic fall in LV pressure (IVR) would be expected to have effects on loop area, in particular when there is pre-ejection or post-ejection shortening. Thus, the pre-ejection septal shortening during LBBB which occurs against low LV pressure, and therefore represents little work, would appear erroneously as a more substantial work if timing of aortic valve opening was set prematurely. Similarly, the work represented by post-systolic shortening in ischemic myocardium would be overestimated if timing of aortic valve closure was set too late. The error in timing of IVC and IVR, however, was minor as demonstrated by testing sensitivity to errors in timing of AVO and AVC.

## Assessing Wasted Work

In paper 4 we introduce wasted work fraction as a novel principle for quantifying function in ventricles with dyssynchronous contraction patterns. The WWF measures how much mechanical energy is used by the ventricle to do work which does not contribute to ejection, and therefore is considered as wasted. Wasted work fraction is total negative work as a fraction of total positive work calculated as a global measure for all segments. The method also gives segmental information about positive and negative work allowing for regional assessment of local energetic efficacy. The strong relation between regional LV pressure-strain loop area and regional myocardial glucose uptake shown previously by our group [37] supports that WWF also reflects a waste in myocardial metabolism and oxygen consumption. Furthermore, we show that wasted work can be measured clinically by an entirely non-invasive approach by combining a non-invasive LV pressure curve with strain by STE. The validity of this method was confirmed in the experimental part of the study. In the clinical study LV work analysis using the non-invasively estimated LV pressure and strain showed that significant work was wasted during LBBB and was subsequently recruited when CRT was introduced, suggesting that the work analysis may represent a means to explore the hemodynamic impact of electrical dyssynchrony and to monitor responses to CRT.

**Wasted work**

In a normal heart, contraction of all segments occur almost simultaneously and they therefore contract against a similar LV pressure. However, in a ventricle with regional differences in timing of contraction, regional contraction occurs against different pressures and information about both the degree of shortening and LV pressure during shortening is therefore needed to compare regional work done by the segments. The same is true for calculation of energy losses during elongation/stretching of a segment, since the energy loss depends on both elongation distance and the instantaneous LV pressure during elongation. In ventricles where timing of relaxation is different between segments, some segments will start relaxing at elevated LV pressure while others are still contracting. This means that a substantial amount of work done by the contracting segments is wasted on stretching of other segments. Measuring wasted work is therefore a method for quantifying work that is being done by the ventricle but does not contribute to LV ejection, and provided the myocardium is viable, should represent a measure of contractile reserve. This was supported by our data in the patient population with LBBB which showed a decrease in WWF and increased ejection fraction when CRT was introduced.

When we are assessing LV function we are interested in quantifying how the myocardium contributes to LV function globally and regionally. Strain imaging has given us a unique tool for this, however, in patients with regional differences in timing of shortening peak strain may not reflect work. Typically, during LBBB much of septal contraction occurs during the pre-ejection phase at a time when the LVP is low, and therefore the septum performs little work. As seen in the present study peak septal strain during LBBB in the animal model is only marginally reduced compared to the lateral wall, but net work done by the septum is approximately one third relative to the lateral wall. In the patients with LBBB peak strain for the septum was on average half of that for the lateral wall which is in keeping with previous studies [47]. Segmental Negative/Positive work ratio, however, was over 1.5, indicating that instead of the septum contributing to the hemodynamic performance of the LV, external work was done on the septum which thereby "absorbed" work done by other segments.

Since the metabolism of myocardial segments is unable to recycle chemical energy when the segments are stretched, this energy will instead be converted to heat in the tissue. Measurements of WWF will for this reason indicate the overall efficacy of the LV myocardium in converting metabolic substrates into cardiac work. A high WWF indicates that the myocardium requires a disproportionately high coronary blood supply.

In summary papers 3 and 4 introduce a novel non-invasive method for work analysis by LV pressure-strain loop areas. Furthermore, we introduce wasted work fraction, a method that

allows for us to quantify how much mechanical energy is used by the ventricle to do work which does not contribute to ejection, and therefore is considered as wasted.

## Limitations

The in vivo experiments in the thesis utilized a heavily instrumented animal model and this preparation may not always represent normal physiology. Although the open-chest condition and instrumentation may have induced some degree of LV dysfunction during baseline, this should not modify the main conclusions from this study. In the in vivo model we investigated isolated mechanical and electrical dyssynchrony. In a clinical situation, however, one may encounter concomitant electrical conduction delay and regional impairment of contractility. The small sample size in the studies may be viewed as a limitation, however, the consistency in our findings support our conclusions.

A limitation of the AFG method is that it requires invasive pressures. However, many patients undergo left heart catheterization as part of a work up prior to CRT and this would give access to LV pressure and pressure-strain loops can be constructed.

Speckle tracking echocardiography measures motion in the image plane while sonomicrometry measures motion of material points in the myocardium. Therefore, a misalignment of the ultrasound plane vs. the crystals may account for some of the discrepancies between the two measurements.

FDG-PET assesses glucose metabolism and will show increased uptake in areas both with aerobic and anaerobic (ischemia) metabolism. Therefore only patients with a normal coronary angiography and no history of coronary artery disease were included. The observed abnormal changes in LV glucose metabolism during LBBB is in keeping with previous findings [48]. The use of a reference curve to define the LV pressure waveform is in principle a limitation of the estimated pressure curve method since patients have different timing of peak LV pressure and the timing varies from time to time in a given patient, however, the good correlation and agreement with invasively measured data support our conclusion.

Strain analysis has limitations, both when using TDI and STE, such as angle dependency and the need for good image quality for the software to track the speckles [49]. All methods described in the present thesis require echocardiographic image quality that allows for strain analysis and are therefore limited to patients were this is possible.

In the present thesis novel methods have been introduced and further studies should be performed to investigate the clinical benefit of onset AFG and work analysis.

## Main conclusions

Through the studies in the present thesis we have made a contribution to the understanding and assessment of dyssynchrony in the heart.

### Paper 1.

Paper 1 demonstrates that onset AFG is an accurate marker of timing of regional electrical activation, allowing for differentiation between primary electrical and primary mechanical dyssynchrony, independent of regional differences in load and contractility. Furthermore, it shows that current indices based on myocardial shortening velocity and strain have significant limitations, and although they measure dyssynchrony, they have limited ability to establish underlying etiology.

### Paper 2.

Prolonged delay from regional electrical activation to onset of shortening in late activated segments during LBBB is due to increased rate of pressure rise (LV dP/dt) at the time of activation. Therefore, a late activated segment needs more time to generate active force at a higher rate than the rise of the applied load (LV dP/dt), which in turn leads to shortening of the segment. The prolonged delay substantially increased mechanical dyssynchrony relative to the underlying electrical dyssynchrony in LBBB patients which implies that shortening indices may overestimate the extent of electrical dyssynchrony in these patients. These findings also suggest that changes in LV contractility may modify mechanical dyssynchrony. We conclude that during LBBB prolonged EMD in late activated myocardium is caused by a higher dP/dt at the time of activation, resulting in aggravated mechanical relative to electrical dyssynchrony. These findings suggest that LV contractility may modify mechanical dyssynchrony.

### Paper 3.

In paper 3 we introduce a novel non-invasive method for LV pressure-strain analysis which may serve as a means to quantify regional myocardial work. Furthermore we show that non-invasive pressure-strain area reflects regional work and metabolism. Assessing work distribution will give the clinician additional information when assessing patients with ischemia and selecting patients for CRT. Work analysis may also play an important part in optimizing CRT settings and improve responder rate.

## Paper 4.

Paper 4 introduces WWF as a non-invasive clinical method to quantify the negative impact of dyssynchrony on myocardial work and energy utilization. Furthermore, we show that significant work was wasted during LBBB and was subsequently recruited when CRT was introduced, suggesting that the work analysis may represent a means to explore the hemodynamic impact of electrical dyssynchrony and to monitor responses to CRT.

# Reference List

Reference List


1. Penicka M, Bartunek J, De BB, Vanderheyden M, Goethals M, De ZM, Brugada P, Geelen P. Improvement of left ventricular function after cardiac resynchronization therapy is predicted by tissue Doppler imaging echocardiography. *Circulation.* 2004;109:978-983.

2. Bader H, Garrigue S, Lafitte S, Reuter S, Jais P, Haissaguerre M, Bonnet J, Clementy J, Roudaut R. Intra-left ventricular electromechanical asynchrony. A new independent predictor of severe cardiac events in heart failure patients. *J Am Coll Cardiol.* 2004;43:248-256.

3. Gorcsan J, III, Abraham T, Agler DA, Bax JJ, Derumeaux G, Grimm RA, Martin R, Steinberg JS, Sutton MS, Yu CM. Echocardiography for cardiac resynchronization therapy: recommendations for performance and reporting--a report from the American Society of Echocardiography Dyssynchrony Writing Group endorsed by the Heart Rhythm Society. *J Am Soc Echocardiogr.* 2008;21:191-213.

4. Epstein AE, DiMarco JP, Ellenbogen KA, Estes NAM, Freedman RA, Gettes LS, Gillinov AM, Gregoratos G, Hammill SC, Hayes DL, Hlatky MA, Newby LK, Page RL, Schoenfeld MH, Silka MJ, Stevenson LW, Sweeney MO. ACC/AHA/HRS 2008 Guidelines for Device-Based Therapy of Cardiac Rhythm Abnormalities. *Circulation.* 2008;117:2820-2840.

5. Cleland JG, Daubert JC, Erdmann E, Freemantle N, Gras D, Kappenberger L, Tavazzi L. The effect of cardiac resynchronization on morbidity and mortality in heart failure. *N Engl J Med.* 2005;352:1539-1549.

6. Bristow MR, Saxon LA, Boehmer J, Krueger S, Kass DA, De MT, Carson P, DiCarlo L, DeMets D, White BG, DeVries DW, Feldman AM. Cardiac-resynchronization therapy with or without an implantable defibrillator in advanced chronic heart failure. *N Engl J Med.* 2004;350:2140-2150.

7. Dickstein K, Vardas PE, Auricchio A, Daubert JC, Linde C, McMurray J, Ponikowski P, Priori SG, Sutton R, van Veldhuisen DJ, Vahanian A, Auricchio A, Bax J, Ceconi C, Dean V, Filippatos G, Funck-Brentano C, Hobbs R, Kearney P, McDonagh T, Popescu BA, Reiner Z, Sechtem U, Sirnes PA, Tendera M, Vardas P, Widimsky P, Tendera M, Anker SD, Blanc JJ, Gasparini M, Hoes AW, Israel CW, Kalarus Z, Merkely B, Swedberg K, Camm AJ. 2010 Focused Update of ESC Guidelines on device therapy in heart failure: an update of the 2008 ESC Guidelines for the diagnosis and treatment of acute and chronic heart failure and the 2007 ESC Guidelines for cardiac and resynchronization therapy. Developed with the special contribution of the Heart Failure Association and the European Heart Rhythm Association. *Europace.* 2010;12:1526-1536.

8. Abraham WT, Fisher WG, Smith AL, Delurgio DB, Leon AR, Loh E, Kocovic DZ, Packer M, Clavell AL, Hayes DL, Ellestad M, Trupp RJ, Underwood J, Pickering F, Truex C, McAtee P, Messenger J, the MIRACLE Study Group. Cardiac Resynchronization in Chronic Heart Failure. *N Engl J Med.* 2002;346:1845-1853.

9. Reuter S, Garrigue S, Barold SS, Jais P, Hocini M, Haissaguerre M, Clementy J. Comparison of characteristics in responders versus nonresponders with biventricular pacing for drug-resistant congestive heart failure. *The American Journal of Cardiology.* 2002;89:346-350.

10. Leclercq C, Faris O, Tunin R, Johnson J, Kato R, Evans F, Spinelli J, Halperin H, McVeigh E, Kass DA. Systolic Improvement and Mechanical Resynchronization Does Not Require Electrical Synchrony in the Dilated Failing Heart With Left Bundle-Branch Block. *Circulation.* 2002;106:1760-1763.

11. Bax JJ, Abraham T, Barold SS, Breithardt OA, Fung JW, Garrigue S, Gorcsan J, III, Hayes DL, Kass DA, Knuuti J, Leclercq C, Linde C, Mark DB, Monaghan MJ, Nihoyannopoulos P, Schalij MJ, Stellbrink C, Yu CM. Cardiac resynchronization therapy: Part 1--issues before device implantation. *J Am Coll Cardiol.* 2005;46:2153-2167.

12. Amundsen BH, Helle-Valle T, Edvardsen T, Torp H, Crosby J, Lyseggen E, Stoylen A, Ihlen H, Lima JA, Smiseth OA, Slordahl SA. Noninvasive myocardial strain measurement by speckle tracking echocardiography: validation against sonomicrometry and tagged magnetic resonance imaging. *J Am Coll Cardiol.* 2006;47:789-793.

13. Edvardsen T, Urheim S, Skulstad H, Steine K, Ihlen H, Smiseth OA. Quantification of left ventricular systolic function by tissue Doppler echocardiography: added value of measuring pre- and postejection velocities in ischemic myocardium. *Circulation.* 2002;105:2071-2077.

14. Wilkenshoff UM, Sovany A, Wigstrom L, Olstad B, Lindstrom L, Engvall J, Janerot-Sjoberg B, Wranne B, Hatle L, Sutherland GR. Regional mean systolic myocardial velocity estimation by real-time color Doppler myocardial imaging: a new technique for quantifying regional systolic function. *J Am Soc Echocardiogr.* 1998;11:683-692.

15. Smiseth OA, Russell K, Skulstad H. The role of echocardiography in quantification of left ventricular dyssynchrony: state of the art and future directions. *Eur Heart J Cardiovasc Imaging.* 2012;13:61-68.

16. Chung ES, Leon AR, Tavazzi L, Sun JP, Nihoyannopoulos P, Merlino J, Abraham WT, Ghio S, Leclercq C, Bax JJ, Yu CM, Gorcsan J, III, St John Sutton M, De Sutter J, Murillo J. Results of the Predictors of Response to CRT (PROSPECT) Trial. *Circulation.* 2008;117:2608-2616.

17. Miyazaki C, Redfield MM, Powell BD, Lin GM, Herges RM, Hodge DO, Olson LJ, Hayes DL, Espinosa RE, Rea RF, Bruce CJ, Nelson SM, Miller FA, Oh JK. Dyssynchrony indices to predict response to cardiac resynchronization therapy: a comprehensive prospective single-center study. *Circ Heart Fail.* 2010;3:565-573.

18. Jessup M, Abraham WT, Casey DE, Feldman AM, Francis GS, Ganiats TG, Konstam MA, Mancini DM, Rahko PS, Silver MA, Stevenson LW, Yancy CW. 2009 focused update: ACCF/AHA Guidelines for the Diagnosis and Management of Heart Failure in Adults: a report of the American College of Cardiology Foundation/American Heart Association Task Force on Practice Guidelines: developed in collaboration with the International Society for Heart and Lung Transplantation. *Circulation.* 2009;119:1977-2016.

19. De Boeck BWL, Meine M, Leenders GE, Teske AJ, van Wessel H, Kirkels JH, Prinzen FW, Doevendans PA, Cramer MJ. Practical and conceptual limitations of tissue Doppler imaging to predict reverse remodelling in cardiac resynchronisation therapy. *European Journal of Heart Failure.* 2008;10:281-290.

20. Leenders GE, Cramer MJ, Bogaard MD, Meine M, Doevendans PA, De Boeck BW. Echocardiographic prediction of outcome after cardiac resynchronization therapy: conventional methods and recent developments. *Heart Fail Rev.* 2011;16:235-250.

21. Suga H. Total mechanical energy of a ventricle model and cardiac oxygen consumption. *Am J Physiol.* 1979;236:H498-H505.

22. Takaoka H, Takeuchi M, Odake M, Yokoyama M. Assessment of myocardial oxygen consumption (Vo2) and systolic pressure-volume area (PVA) in human hearts. *Eur Heart J.* 1992;13 Suppl E:85-90.

23. Hisano R, Cooper G. Correlation of force-length area with oxygen consumption in ferret papillary muscle. *Circ Res.* 1987;61:318-328.

24. Tyberg JV, Forrester JS, Wyatt HL, Goldner SJ, Parmley WW, Swan HJ. An analysis of segmental ischemic dysfunction utilizing the pressure-length loop. *Circulation.* 1974;49:748-754.

25. Forrester JS, Tyberg JV, Wyatt HL, Goldner S, Parmely WW, Swan HJ. Pressure-length loop: a new method for simultaneous measurement of segmental and total cardiac function. *J Appl Physiol.* 1974;37:771-775.

26. Delhaas T, Arts T, Prinzen FW, Reneman RS. Regional fibre stress-fibre strain area as an estimate of regional blood flow and oxygen demand in the canine heart. *J Physiol.* 1994;477 ( Pt 3):481-496.

27. Urheim S, Rabben SI, Skulstad H, Lyseggen E, Ihlen H, Smiseth OA. Regional myocardial work by strain Doppler echocardiography and LV pressure: a new method for quantifying myocardial function. *Am J Physiol Heart Circ Physiol.* 2005;288:H2375-H2380.

28. Prinzen FW, Hunter WC, Wyman BT, McVeigh ER. Mapping of regional myocardial strain and work during ventricular pacing: experimental study using magnetic resonance imaging tagging. *J Am Coll Cardiol.* 1999;33:1735-1742.

29. Prinzen FW, Cheriex EC, Delhaas T, van Oosterhout MFM, Arts T, Wellens HJJ, Reneman RS. Asymmetric thickness of the left ventricular wall resulting from asynchronous electric activation: A study in dogs with ventricular pacing and in patients with left bundle branch block. *American Heart Journal.* 1995;130:1045-1053.

30. van Oosterhout MFM, Arts T, Muijtjens AMM, Reneman RS, Prinzen FW. Remodeling by ventricular pacing in hypertrophying dog hearts. *Cardiovasc Res.* 2001;49:771-778.

31. Ukkonen H, Beanlands RS, Burwash IG, de Kemp RA, Nahmias C, Fallen E, Hill MR, Tang AS. Effect of cardiac resynchronization on myocardial efficiency and regional oxidative metabolism. *Circulation.* 2003;107:28-31.

32. Prinzen FW, Augustijn CH, Arts T, Allessie MA, Reneman RS. Redistribution of myocardial fiber strain and blood flow by asynchronous activation. *Am J Physiol.* 1990;259:H300-H308.

33. van Oosterhout MF, Prinzen FW, Arts T, Schreuder JJ, Vanagt WY, Cleutjens JP, Reneman RS. Asynchronous electrical activation induces asymmetrical hypertrophy of the left ventricular wall. *Circulation.* 1998;98:588-595.

34. Gjesdal O, Remme EW, Opdahl A, Skulstad H, Russell K, Kongsgaard E, Edvardsen T, Smiseth OA. Mechanisms of abnormal systolic motion of the interventricular septum during left bundle-branch block. *Circ Cardiovasc Imaging.* 2011;4:264-273.

35. Urheim S, Edvardsen T, Torp H, Angelsen B, Smiseth OA. Myocardial Strain by Doppler Echocardiography : Validation of a New Method to Quantify Regional Myocardial Function. *Circulation.* 2000;102:1158-1164.

36. Russell K, Opdahl A, Remme EW, Gjesdal O, Skulstad H, Kongsgaard E, Edvardsen T, Smiseth OA. Evaluation of left ventricular dyssynchrony by onset of active myocardial force generation: a novel method that differentiates between electrical and mechanical etiologies. *Circ Cardiovasc Imaging.* 2010;3:405-414.

37. Russell K, Eriksen M, Aaberge L, Wilhelmsen N, Skulstad H, Remme EW, Haugaa KH, Opdahl A, Fjeld JG, Gjesdal O, Edvardsen T, Smiseth OA. A novel clinical method for quantification of regional left ventricular pressure-strain loop area: a non-invasive index of myocardial work. *Eur Heart J.* 2012;33:724-733.

38. Russell K, Smiseth OA, Gjesdal O, Qvigstad E, Norseng PA, Sjaastad I, Opdahl A, Skulstad H, Edvardsen T, Remme EW. Mechanism of prolonged electromechanical delay in late activated

myocardium during left bundle branch block. *Am J Physiol Heart Circ Physiol.* 2011;301:H2334-H2343.

39. Martin WH, Jones RC, Delbeke D, Sandler MP. A simplified intravenous glucose loading protocol for fluorine-18 fluorodeoxyglucose cardiac single-photon emission tomography. *Eur J Nucl Med.* 1997;24:1291-1297.

40. Bland JM, Altman DG. Agreement between methods of measurement with multiple observations per individual. *J Biopharm Stat.* 2007;17:571-582.

41. Ruffy R, Lovelace DE, Mueller TM, Knoebel SB, Zipes DP. Relationship between changes in left ventricular bipolar electrograms and regional myocardial blood flow during acute coronary artery occlusion in the dog. *Circ Res.* 1979;45:764-770.

42. Prinzen FW, Augustijn CH, Allessie MA, Arts T, Delhaas T, Reneman RS. The time sequence of electrical and mechanical activation during spontaneous beating and ectopic stimulation. *Eur Heart J.* 1992;13:535-543.

43. Gamble J, Taylor PB, Kenno KA. Myocardial stretch alters twitch characteristics and Ca2+ loading of sarcoplasmic reticulum in rat ventricular muscle. *Cardiovasc Res.* 1992;26:865-870.

44. Skulstad H, Edvardsen T, Urheim S, Rabben SI, Stugaard M, Lyseggen E, Ihlen H, Smiseth OA. Postsystolic shortening in ischemic myocardium: active contraction or passive recoil? *Circulation.* 2002;106:718-724.

45. Bergman BC, Tsvetkova T, Lowes B, Wolfel EE. Myocardial glucose and lactate metabolism during rest and atrial pacing in humans. *J Physiol.* 2009;587:2087-2099.

46. Prinzen FW, Hunter WC, Wyman BT, McVeigh ER. Mapping of regional myocardial strain and work during ventricular pacing: experimental study using magnetic resonance imaging tagging. *J Am Coll Cardiol.* 1999;33:1735-1742.

47. Klimusina J, De Boeck BW, Leenders GE, Faletra FF, Prinzen F, Averaimo M, Pasotti E, Klersy C, Moccetti T, Auricchio A. Redistribution of left ventricular strain by cardiac resynchronization therapy in heart failure patients. *Eur J Heart Fail.* 2011;13:186-194.

48. Nowak B, Sinha AM, Schaefer WM, Koch KC, Kaiser HJ, Hanrath P, Buell U, Stellbrink C. Cardiac resynchronization therapy homogenizes myocardial glucose metabolism and perfusion in dilated cardiomyopathy and left bundle branch block. *J Am Coll Cardiol.* 2003;41:1523-1528.

49. Mor-Avi V, Lang RM, Badano LP, Belohlavek M, Cardim NM, Derumeaux G, Galderisi M, Marwick T, Nagueh SF, Sengupta PP, Sicari R, Smiseth OA, Smulevitz B, Takeuchi M, Thomas JD, Vannan M, Voigt JU, Zamorano JL. Current and evolving echocardiographic techniques for the quantitative evaluation of cardiac mechanics: ASE/EAE consensus statement on methodology and indications endorsed by the Japanese Society of Echocardiography. *Eur J Echocardiogr.* 2011;12:167-205.

# Paper 1

# Paper 2

# Paper 3

European Heart Journal Advance Access published February 18, 2012

European Heart Journal
doi:10.1093/eurheartj/ehs016

FASTTRACK
CLINICAL RESEARCH

# A novel clinical method for quantification of regional left ventricular pressure–strain loop area: a non-invasive index of myocardial work

**Kristoffer Russell[1,2,3], Morten Eriksen[1,3], Lars Aaberge[2,3], Nils Wilhelmsen[2], Helge Skulstad[1,2], Espen W. Remme[1,3,4], Kristina H. Haugaa[1,2,3], Anders Opdahl[1,2], Jan Gunnar Fjeld[5], Ola Gjesdal[1,2], Thor Edvardsen[1,2,3], and Otto A. Smiseth[1,2,3]***

[1]Institute for Surgical Research, Oslo University Hospital, Rikshospitalet, University of Oslo, Oslo, Norway; [2]Department of Cardiology, Oslo University Hospital, Rikshospitalet, University of Oslo, N-0027 Oslo, Norway; [3]Center for Cardiological Innovation, Oslo University Hospital, University of Oslo, Oslo, Norway; [4]KG Jebsen Cardiac Research Centre, Oslo, Norway; and [5]Department of Radiology and Nuclear Medicine, Oslo University Hospital, University of Oslo, Oslo, Norway

*Received 9 November 2011; revised 22 December 2011; accepted 16 January 2012*

**Aims** Left ventricular (LV) pressure–strain loop area reflects regional myocardial work and metabolic demand, but the clinical use of this index is limited by the need for invasive pressure. In this study, we introduce a non-invasive method to measure LV pressure–strain loop area.

**Methods and results** Left ventricular pressure was estimated by utilizing the profile of an empiric, normalized reference curve which was adjusted according to the duration of LV isovolumic and ejection phases, as defined by timing of aortic and mitral valve events by echocardiography. Absolute LV systolic pressure was set equal to arterial pressure measured invasively in dogs ($n = 12$) and non-invasively in patients ($n = 18$). In six patients, myocardial glucose metabolism was measured by positron emission tomography (PET). First, we studied anaesthetized dogs and observed an excellent correlation ($r = 0.96$) and a good agreement between estimated LV pressure–strain loop area and loop area by LV micromanometer and sonomicrometry. Secondly, we validated the method in patients with various cardiac disorders, including LV dyssynchrony, and confirmed an excellent correlation ($r = 0.99$) and a good agreement between pressure–strain loop areas using non-invasive and invasive LV pressure. Non-invasive pressure–strain loop area reflected work when incorporating changes in local LV geometry ($r = 0.97$) and showed a strong correlation with regional myocardial glucose metabolism by PET ($r = 0.81$).

**Conclusions** The novel non-invasive method for regional LV pressure–strain loop area corresponded well with invasive measurements and with directly measured myocardial work and it reflected myocardial metabolism. This method for assessment of regional work may be of clinical interest for several patients groups, including LV dyssynchrony and ischaemia.

**Keywords** Heart failure • Dyssynchrony • Cardiac resynchronization therapy

## Introduction

Clinical assessment of left ventricular (LV) systolic function is commonly performed by measuring indices of myocardial fibre shortening such as LV ejection fraction which is a global index, and LV wall thickening, myocardial velocity, and strain which reflect regional function. The shortening indices, however, do not reflect myocardial work or oxygen demand. As shown by Suga[1] in an experimental study, the area of the LV pressure–volume loop reflects stroke work as well as myocardial oxygen consumption, and it was later confirmed that this concept is valid clinically.[2] According to the same principle, the area of the myocardial force–segment length loop reflects regional myocardial work and oxygen consumption.[3] Because calculation of myocardial force is challenging, pressure is used as a substitute for force and the area of LV pressure–dimension loop is used as an index of regional work.[4–7]

In the present study, we introduce a non-invasive method for LV work analysis which is based upon an estimated LV pressure curve

* Corresponding author. Tel: +47 23070000/+47 23073271, Fax: +47 23073917, Email: osmiseth@ous-hf.no

in combination with strain by speckle-tracking echocardiography (STE). The estimated pressure curve is generated by adjusting the profile of a reference LV pressure curve according to the duration of the isovolumic and ejection phases as measured by echocardiographic timing of aortic and mitral valve events. Peak LV pressure was estimated non-invasively from brachial artery cuff pressure. The main objective of the present study was to determine whether LV pressure–strain loop area can be estimated with an entirely non-invasive approach by using the estimated pressure curve in combination with strain by STE. First, we tested the principle in a dog model under a wide range of haemodynamic conditions with LV micromanometer and implanted ultrasonic dimension crystals as reference methods. Secondly, we validated the non-invasive method in patients and used invasive LV pressure in combination with strain by STE as a reference method for pressure–strain loop area. Finally, to determine whether pressure–strain loop area reflects regional myocardial metabolism, we compared loop area with glucose turnover measured by positron emission tomography (PET).

# Methods

## Experimental study

### Animal preparation

Twelve mongrel dogs of either sex and body weight 36 ± 2 kg were anaesthetized, ventilated, and surgically prepared as previously described,[7] including induction of left bundle branch block (LBBB, $n = 6$) by radiofrequency ablation[8] and regional ischaemia ($n = 6$) by left anterior descending coronary artery (LAD) occlusion. The study was approved by the National Animal Experimentation Board. The laboratory animals were supplied by Centre for Comparative Medicine, Oslo University Hospital, Rikshospitalet, Norway.

### Haemodynamic measurements and sonomicrometry

Ascending aortic pressure, left atrial pressure, and LV pressure (LVP) were measured by micromanometers (MPC-500, Millar Instruments Inc., Houston, TX, USA). Segment lengths were measured using sonomicrometry crystals implanted endocardially (Sonometrics Corp., London, Ontario, Canada). In dogs with LBBB, longitudinal crystal pairs were placed in the septum and LV lateral wall, and a circumferential pair was placed in the posterolateral LV free wall. In the ischaemia group, a longitudinal pair was placed in the perfusion territory of the LAD. Strain was calculated as the percentage of end-diastolic length. Data were sampled at 200 Hz.

### Echocardiography

A Vivid 7 ultrasound scanner (GE Vingmed Ultrasound AS, Horten, Norway) was used to record two-dimensional (2D) grey-scale images and strain by STE. Recordings were done in the LV equatorial short-axis and two- and four-chamber views (frame rate 63 ± 13 $s^{-1}$), and recordings were also done corresponding to the location of ultrasound crystals. Strain was measured successfully at all interventions, except for one dog during ischaemia.

### Experimental protocol

In six dogs, measurements were performed at baseline and after induction of LBBB. In the remaining six animals, recordings were done before and after LAD occlusion for 60 min. Data were recorded with the ventilator temporarily switched off.

## Clinical study

The study population included 24 patients with mean age 66 ± 8 years (25% females). All patients had chronic heart failure (NYHA II–IV). A total of 18 patients underwent LV catheterization, including 11 with ischaemic cardiomyopathy and 7 with non-ischaemic dilated cardiomyopathy. Twelve of these patients had LBBB (QRS 160 ± 20 ms). Two of the patients with LBBB had a cardiac resynchronization therapy (CRT) device allowing for measurements with CRT on and off.

The six remaining patients were studied with $^{18}$F-fluorodeoxyglucose PET imaging (FDG-PET). These patients had dilated cardiomyopathy and LBBB (QRS 165 ± 16 ms). Coronary artery disease was ruled out by coronary angiography. In these patients, only the non-invasively estimated pressure curve was used for calculation of work. The study was approved by the Regional Committee for Medical Research Ethics. All subjects gave written informed consent.

### Haemodynamic and echocardiographic measurements

Left ventricular pressure was measured by a micromanometer-tipped catheter (Millar) and a fluid-filled catheter connected to an external pressure transducer served as an absolute pressure reference. Brachial artery cuff pressure was measured. Myocardial strain was measured by STE in apical long-axis and two- and four-chamber views (frame rate 67 ± 7 $s^{-1}$), and 2D images with a narrow sector over the valves (frame rate 91 ± 23 $s^{-1}$) were used to define opening and closure of the aortic and mitral valves. Pressure and strain data were recorded in a synchronized fashion and stored on the scanner for offline analysis. Echocardiography was performed immediately after the PET study. Patients with echocardiography images not amenable for speckle tracking were excluded prior to invasive pressure measurements ($n = 2$). An average of 16 ± 2 segments were analysed in each patient.

### Fluorodeoxyglucose positron emission tomography

To reduce myocardial fatty acid metabolism and stimulate insulin-dependent glucose uptake, plasma glucose levels were titrated with oral glucose and i.v. insulin as described previously.[9] Gated FDG-PET acquisition (Simens Biograph 64) was started 60–80 min after i.v. administration of the FDG (370–380 MBq), with eight gates per RR interval. The acquisition was also gated for respiration. Images were reconstructed and analysed on the Xeleris workstation (GE Healthcare). The point in the LV myocardium with the highest FDG uptake was used as a reference (100%), and segmental values were reported as percentages of this value.

## Calculation of estimated left ventricular pressure curve

The non-invasively estimated LV pressure curve was validated first in the dog model which allowed testing under a wide range of haemodynamic conditions. Thereafter, the method was validated in patients with various cardiac disorders. As an estimate of peak LV pressure, aortic pressure measured invasively was used in dogs and brachial artery cuff pressure in patients. The profile of the estimated LV pressure curve was determined by using an empiric reference curve which was adjusted according to the duration of the isovolumic and ejection phases as determined by echocardiography.

### Calculating left ventricular pressure reference curve

The LV pressure reference curve was calculated by pooling single cycle LV pressure traces from all interventions and normalizing each pressure trace using timing of valvular events in the following three steps: (i) the timing of opening and closure of the mitral and aortic valves was identified by echocardiography and assigned to each of

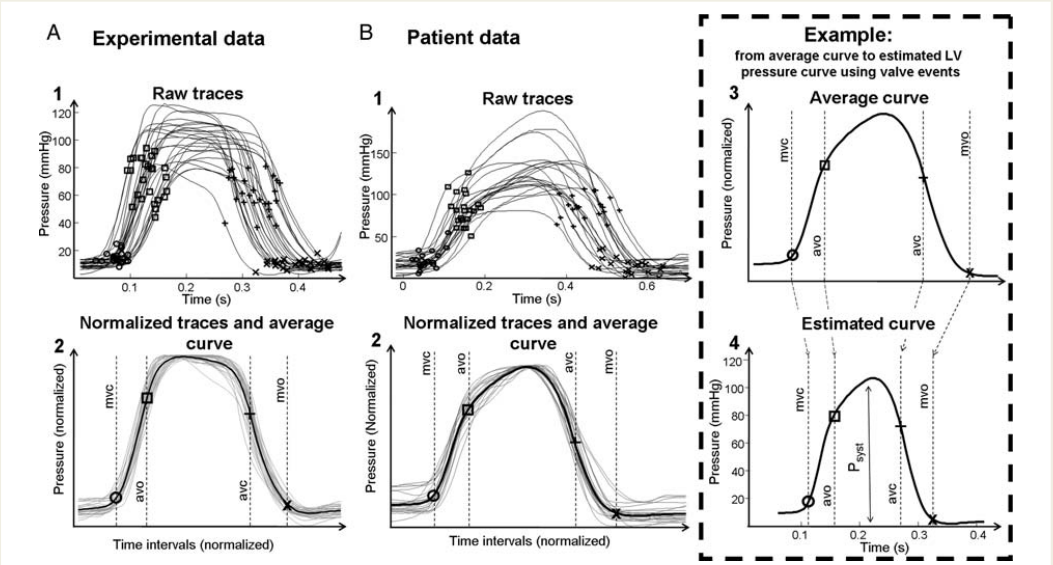


**Figure 1** Estimation of left ventricular pressure curve. (*A*, 1) Raw left ventricular pressure data from dogs used for creating a profile of the reference pressure waveform, consisting of pressure recordings under different haemodynamic situations. Timing of mitral and aortic valve events is indicated. (*A*, 2) The raw pressure waveforms (grey curves) have been stretched or compressed along the time axis between individual valve events in order to make the valvular events coincide for all recordings. The waveforms have also been vertically scaled to have the same peak value. The averaged waveform to be used for predicting pressure traces is indicated by the black curve. (*B*, 1 and 2) Patient data: estimation of average pressure waveform as described in (*A*, 1) and (*A*, 2). (*B*, 3) The averaged waveform with arbitrary time intervals, transferred from (*B*, 2). (*B*, 4) Prediction of the left ventricular pressure waveform is based on the timing of valvular event. The left ventricular pressure waveform is constructed by adjusting the duration of time intervals to match the actual valvular timing as determined by echocardiography in the specific subject. In addition to the time-axis adjustments, the waveform has been scaled according to systolic arterial cuff pressure.

the pressure traces (*Figure 1A*1 and *B*1). (ii) Each of the raw data traces was stretched or compressed along the time axis between individual valve events in order to make the valvular events coincide for all recordings (*Figure 1*A2 and *B*2). (iii) All traces were scaled vertically to have the same peak value. An averaged waveform was then calculated (black line in *Figure 1*A2 and *B*2).

### Applying left ventricular pressure reference curve to a specific subject

The reference curve was used for predicting LVP in a specific subject by measuring the actual valvular timing and adjusting the duration of time intervals of isovolumic contraction (IVC), ejection, and isovolumic relaxation (IVR) phases by stretching or compressing the time axis of the averaged LV pressure curve to match the measured time intervals (*Figure 1B*3 and 4). Peak arterial pressure was used to scale the amplitude of the pressure curve. Separate reference curves were used for dogs and patients. Note that data from all interventions in the dog study were used and that data from all patient observations were included in the calculation of the normalized LV pressure reference curve without considering their clinical status.

## Data analysis: experimental study

Strain and pressure data were synchronized using onset R in electrocardiogram as a common time reference. Strain by STE was converted to the same sampling rate as sonomicrometry (200 Hz) by bandlimited sinc interpolation. Loop area was calculated by the following methods:

(i) *Invasive method*. The area of the LV pressure–strain loops by LVP and STE.
(ii) *Non-invasive method*. The area of the LV pressure–strain loops by the estimated LV pressure curve and STE.

### Comparison between left ventricular pressure–strain loop area and myocardial work

Left ventricular pressure–strain loop area as an index and myocardial work does not take into account effects on work related to changes in the radius of curvature or contribution from different fibre directions. To determine the magnitude of this effect, we measured myocardial work incorporating LV geometry (circumferential and longitudinal) and area strain during LBBB (for methods described in detail, see Supplementary material online, *Appendix S1*). To be able to compare the two methods, we correlated work done by the septum divided by work done by the lateral wall using the two methods. A comparison between the septum and the lateral wall was made because during LBBB, the septum does less work compared with the lateral wall.

### Statistical analysis

Values are expressed as mean ± SD. Variables were compared using least-squares linear regression, Pearson's correlation coefficients, and the Bland–Altman plots with calculations of limits of agreement. To

**Table 1 Haemodynamic variables and loop areas in experimental study**

| | LBBB group | | | | Ischaemia group | |
|---|---|---|---|---|---|---|
| | Baseline ($n = 6$) | | LBBB ($n = 6$) | | Baseline ($n = 6$) | Ischaemia ($n = 6$) |
| Haemodynamic variables and ECG | | | | | | |
| Heart rate (b.p.m.) | 121 ± 17 | | 122 ± 13 | | 107 ± 16 | 134 ± 9* |
| QRS width (ms) | 68 ± 5 | | 116 ± 7* | | 69 ± 9 | 67 ± 8 |
| LV $dP/dt_{max}$ (mmHg/s) | 1284 ± 198 | | 1098 ± 189 | | 1794 ± 337 | 1737 ± 102 |
| LV EDP (mmHg) | 10 ± 3 | | 10 ± 4 | | 8 ± 1 | 10 ± 2 |
| Peak LVP (mmHg) | 96 ± 12 | | 94 ± 9 | | 111 ± 11 | 114 ± 9 |
| Loop areas | | | | | | |
| | **Septum** | **Lateral wall** | **Septum** | **Lateral wall** | **Anterior wall** | **Anterior wall** |
| Invasive method | | | | | | |
| Loop area by LV pressure–strain (mmHg %) | 693 ± 256 | 659 ± 264 | 155 ± 289* | 1024 ± 486* | 932 ± 239 | 322 ± 250* |
| Non-invasive method | | | | | | |
| Loop area by estimated LV pressure–strain (mmHg %) | 839 ± 230 | 770 ± 269 | 227 ± 278* | 1031 ± 475* | 914 ± 242 | 295 ± 221* |

Values are mean ± SD. LBBB, left bundle branch block; EDP, end-diastolic pressure; anterior wall affected by ischaemia. Strain was measured by speckle tracking echocardiography.
*$P < 0.05$ vs. baseline.

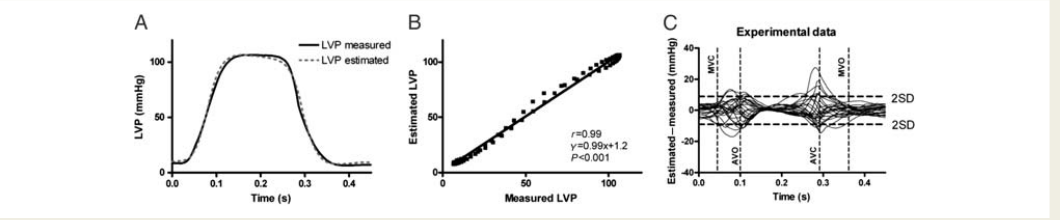


**Figure 2** Comparison between estimated and measured left ventricular pressure. (*A*) Traces from a representative dog. (*B*) Point-for-point correlation between measured left ventricular pressure and the estimated left ventricular pressure curve for the same animal as in (*A*). (*C*) There was good agreement between measured left ventricular pressure vs. estimated left ventricular pressure as a function of time for all the animals (limits of agreement −8.9–8.9 mmHg).

account for multiple measurements from each animal or patient when using the Bland–Altman plots, we display reference intervals based on agreement between methods of measurement with multiple observations per individual.[10] For multiple comparisons, we used two-way repeated-measurements ANOVA with least significant difference post-test (SPSS 15.0, SPSS Inc., Chicago, IL, USA). All *post hoc* tests are compared with baseline. A value of $P < 0.05$ was considered significant.

To assess interobserver variability, loop area using estimated LV pressure for six randomly selected patients was analysed by two independent observers, using the interclass correlation coefficient ($\alpha$ value) and the Bland–Altman method.

# Results

## Experimental study

Haemodynamic variables at baseline, LBBB, and LAD occlusion are displayed in *Table 1*. There was a strong correlation between measured LVP and the estimated LV pressure curve for all animals during all interventions with mean $r = 0.99$ (range 0.98–1.0; *Figure 2A* and *B*). *Figure 2C* shows a good agreement between measured LV pressure vs. the estimated LV pressure curve as a function of time (limit of agreement −8.9–8.9 mmHg).

### Pressure–strain loops

When comparing the areas of the pressure–strain loops using the estimated LV pressure curve and the LV pressure–segment length loop, there was an excellent correlation ($r = 0.96$) and a good agreement (*Figure 3A* and *B*). There was also an excellent correlation ($r = 0.99$) and a good agreement between areas of the pressure–strain loop using the estimated LV pressure curve and the pressure–strain loops using measured LVP (*Figures 4A* and *5A* and *B*). Induction of LBBB was associated with a marked decrease in LV pressure–strain loop area in the septum and there was an

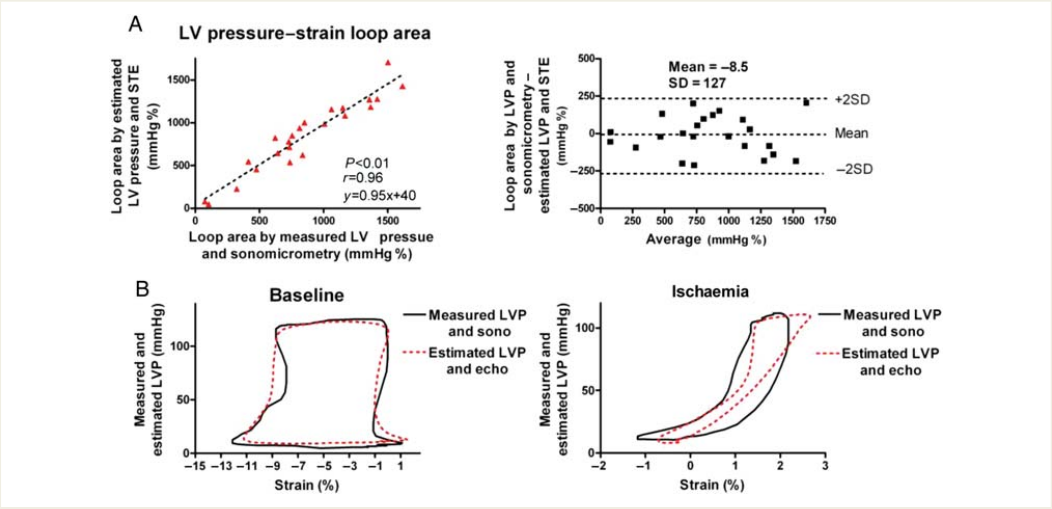


**Figure 3** (*A*) Correlation and agreement between area of the pressure–strain loops by estimated left ventricular pressure and speckle tracking echocardiography vs. measured left ventricular pressure and sonomicrometry. (*B*) Representative traces showing pressure–strain loops by left ventricular pressure and sonomicrometry (black line) vs. estimated left ventricular pressure and echocardiography (red dotted line). Measurements during baseline (left panel) and ischaemia (right panel). Sono, sonomicrometry; echo, speckle tracking echocardiography.

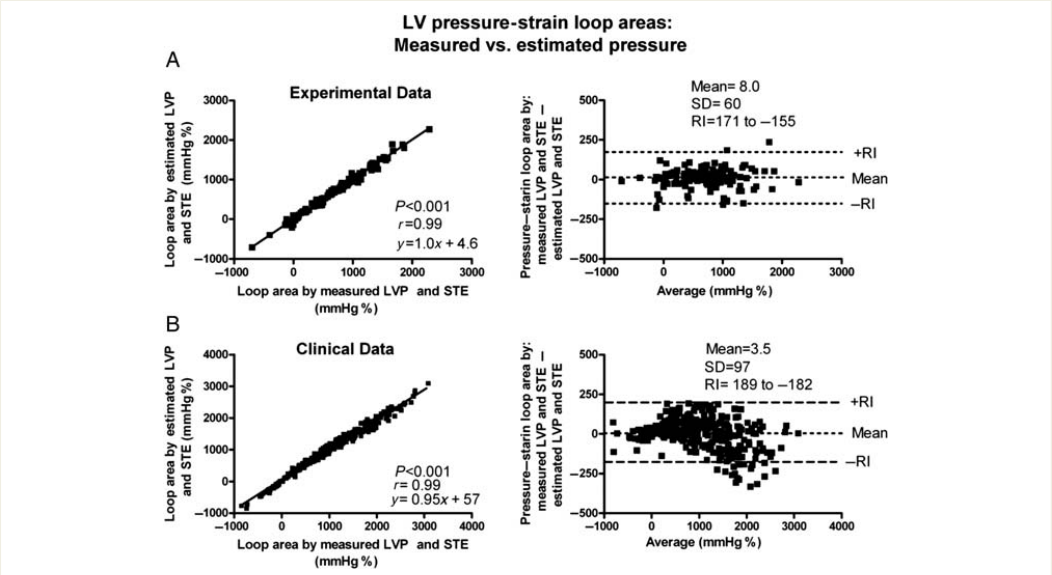


**Figure 4** Correlation and agreement between area of the pressure–strain loops by estimated left ventricular pressure and speckle tracking echocardiography (STE) vs. measured left ventricular pressure and STE. (*A*) Experimental data. (*B*) Clinical data. Note that the same strain data are used for calculation by the two methods to show the isolated variation in loop area by using the non-invasive left ventricular pressure curve vs. measured left ventricular pressure. RI, reference interval.

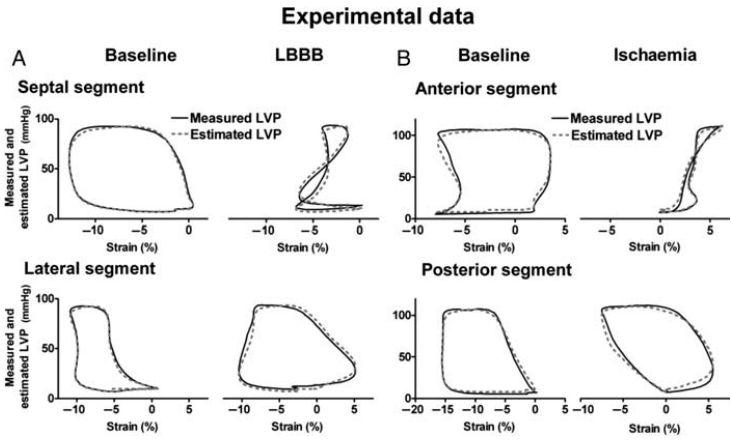


**Figure 5** Representative traces showing pressure–strain loops by left ventricular pressure and speckle-tracking echocardiography (solid line) vs. estimated left ventricular pressure and speckle-tracking echocardiography (dashed line). Measurements during baseline and left bundle branch block (*A*) and during baseline and ischaemia (*B*) in the experimental dog model.

increase in loop area in the LV lateral wall (*Figure 5A* and *Table 1*). As predicted, the LV pressure–strain loop area decreased significantly in the segments affected by ischaemia compared with baseline (*Figures 3B* and *5B*, and *Table 1*).

### Relationship between myocardial work and pressure–strain loop area during LBBB

Induction of LBBB was associated with flattening of the septum relative to the lateral wall. This was expressed as a decrease in mean systolic curvature for the septum relative to the LV free wall: reduction in septal curvature/reduction in lateral wall curvature = 1.14. Furthermore, work done by the septum relative to the lateral wall was greater when calculated using curvature data and area–strain compared with calculations done using the non-invasive method with ratios of 0.54 ± 0.60 and 0.43 ± 0.67, respectively, but these differences were not statistically significant ($P = 0.202$). There was, however, an excellent correlation between the two methods ($r = 0.97$, $y = 0.73x + 0.15$, $P < 0.0001$) when comparing relative values between the septum and the LV lateral wall.

## Clinical study

The patients had a QRS width of 140 ± 40 ms, a peak LVP of 128 ± 22 mmHg, and a heart rate of 73 ± 29 b.p.m. The peak brachial systolic pressure was 131 ± 19 mmHg.

### Left ventricular pressure–strain loops

There was an excellent correlation ($r = 0.99$) and a good agreement between areas of the pressure–strain loops using measured and estimated LV pressure (*Figure 4B*). Similar to observations in the experimental study, patients with LBBB demonstrated markedly reduced work in the septum compared with the lateral wall (358 ± 512 vs. 1308 ± 495 and 402 ± 539 vs.1315 ± 473 mmHg %, by the invasive and non-invasive methods, respectively). Pressure–strain loops from a representative patient are displayed in *Figure 6* and show how CRT alters loop areas. Also in the ischaemic cardiomyopathy patients without LBBB, findings were similar to those in the experimental study. The pressure–strain loop area was significantly reduced in areas supplied by an occluded coronary artery compared with areas with normal perfusion assessed by angiography (248 ± 629 vs.1181 ± 626 and 223 ± 636 vs.1186 ± 583, by the invasive and non-invasive methods, respectively).

### Relationship between myocardial glucose metabolism (fluorodeoxyglucose positron emission tomography) and pressure–strain loop area during left bundle branch block

Glucose metabolism in the patients with LBBB showed significant regional differences and was highest in the lateral wall and lowest in the septum. The non-invasive LV pressure–strain loop area showed a pattern of regional work distribution which was very similar to the distribution of glucose uptake (*Figure 7*). The correlation between segmental values of the loop area and FDG uptake for all the patients was strong with average $r = 0.81$ and individual values ranging from 0.70 to 0.87.

### Interobserver variability

Measurements of 22 loop areas by two independent observers showed a mean difference of −46 mmHg % with an average loop area of 765 mmHg %. The intraclass correlation coefficient between the two observers was 0.99, indicating good reproducibility.

# Discussion

In the present study, we demonstrate that LV pressure–strain loop area, which reflects regional LV myocardial work, can be measured

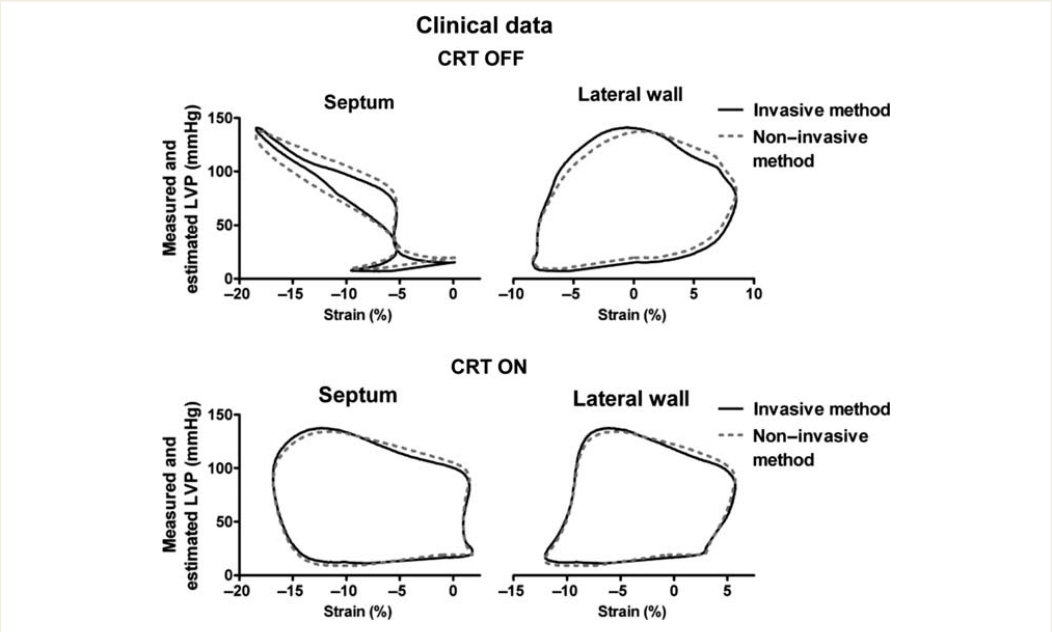


**Figure 6** Loop areas by left ventricular pressure and speckle-tracking echocardiography (solid line) vs. the non-invasive method by estimated left ventricular pressure and speckle-tracking echocardiography (dashed line), for a septal and lateral wall segment in a patient with the cardiac resynchronization therapy device turned on and off.

clinically by an entirely non-invasive approach. This was feasible by combining a non-invasively estimated LV pressure curve with strain by STE. The validity of this method was confirmed in the experimental part of the study by an excellent correlation and a good agreement with loop area by invasive pressure–segment length analysis. In the clinical study, LV pressure–strain loop area using the non-invasive LV pressure curve showed a strong correlation and a good agreement with loop area using invasive LV pressure. When the non-invasive pressure–strain assessment was applied in patients with LBBB, we observed a marked non-uniformity in work distribution with reduced work in the septum and increased work in the LV lateral wall, suggesting that the work analysis may represent a means to explore the haemodynamic impact of electrical dyssynchrony and to monitor responses to CRT. Non-uniformity in work distribution was also apparent when comparing ischaemic vs. non-ischaemic segments. Furthermore, we show that non-invasive pressure–strain loop area reflects regional metabolism, which further supports its use as an index of myocardial work.

## Calculation of work

In principle, the area of the myocardial force–dimension loop represents regional LV work and may also be used as a mechanical index of regional myocardial oxygen consumption.[3] Regional work by force–dimension analysis can be measured in animal preparations using LV pressure in combination with sonomicrometry or cardiac magnetic resonance imaging and by taking local geometry into consideration.[11,12] There is, however, no easily accessible clinical method to record myocardial force–dimension loops since calculation of force requires measurements which are difficult to obtain simultaneously and continuously throughout the heart cycle. In the present study, we used pressure as a substitute for force and the area of the LV pressure–strain loop was used as an index of regional work. This index does not provide a measure, which has units of work, and does not incorporate the modifying effect of local radii of curvature or contributions from different fibre orientations on force. To address these issues and in particular to explore how changes in septal curvature during LBBB would modify the ability of septal pressure–strain loop area to reflect the force–strain loop area, we performed additional analysis. This analysis showed that induction of LBBB was associated with a decrease in mean systolic (circumferential and longitudinal) curvature for both the septum and the lateral wall, compared with baseline. Although the septum flattens during LBBB as a result of its initial rapid contraction during IVC,[8] the relative difference in mean systolic curvature between the septum and the lateral wall was not statistically significant because after this initial contraction, the septum was stretched and maintained its curvature during ejection relative to the lateral wall. We also observed a tendency, although not significant, that the relative difference in work done by the septum compared with the lateral wall was greater when calculated using curvature data and area–strain compared with

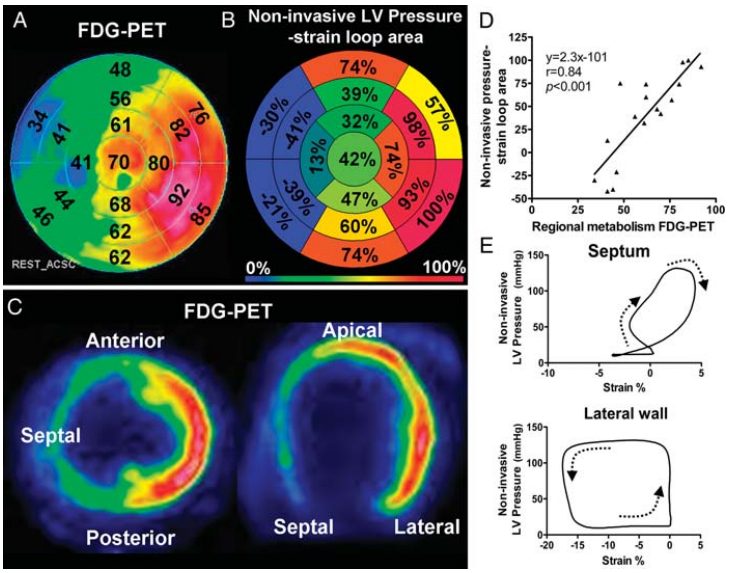


**Figure 7** Data from one representative patient. (*A*) Bull's eye plot showing relative glucose metabolism by fluorodeoxyglucose positron emission tomography (FDG-PET) in a representative patient with left bundle branch block. The point in the left ventricular myocardium with the highest FDG uptake was used as a reference (100%), and segmental values were reported as percentages of this value. (*B*) Bull's eye plot with similar anatomical distribution as in (*A*), showing relative loop area by estimated left ventricular pressure and speckle-tracking echocardiography. The segment with the largest loop area was used as a reference (100%), and segmental values were reported as percentages of this value. (*C*) Correlation between regional metabolism by FDG-PET and loop area by estimated left ventricular pressure and speckle-tracking echocardiography. (*D*) Representative pictures showing regional distribution of glucose metabolism by FDG-PET for short-axis (left panel) and four-chamber (right panel) views. (*E*) Estimated left ventricular pressure and speckle-tracking echocardiography loops from the septum and lateral wall.

calculations done using pressure–strain loop area. However, there was a strong correlation between relative work using the two methods ($r = 0.97$), indicating that the pressure–strain loop area gives adequate clinical information regarding relative differences in work distribution within the same heart. Furthermore, in our laboratory, we have previously demonstrated that changes in segmental pressure–dimension loops approximate changes in the stress–dimension loops during myocardial ischaemia.[13]

The ability of pressure length area to reflect myocardial oxygen consumption has been shown previously.[6] In the present study, we found that the non-invasive LV pressure–strain loop area had a strong correlation and agreement with regional glucose metabolism using FDG-PET. Previous studies have shown that glucose metabolism reflects myocardial work,[14] and this finding therefore supports our conclusion that pressure–strain loop area reflects differences in myocardial work distribution. The present findings of regional changes in work distribution in patients with LBBB are in keeping with the observations by Prinzen *et al.*[12] in a dog model with right ventricular pacing.

## Estimated left ventricular pressure curve

There are numerous techniques which can provide a more accurate central aortic pressure than just using brachial artery cuff pressure, and these may be applied in combination with the present method. However, when the non-invasive pressure method is used for comparing work between segments, the main issue is the abnormal distribution of work and not the absolute values.

It is important to note that the only application of the non-invasive pressure curve proposed in this study was to serve as a pressure estimate when calculating LV pressure–strain loop areas, and for this application, it served its purpose very well, as indicated by the excellent relationship to reference methods for pressure loop area. It does not have sufficient accuracy, however, to provide a measure of LV diastolic pressure or peak rate of rise or fall in LV pressure.

Whereas correct timing of peak LV pressure was of little importance for pressure–strain loop area, errors in timing of early systolic rise in pressure (IVC) and early-diastolic fall in LV pressure (IVR) would be expected to have effects on loop area, in particular when there is pre-ejection or post-ejection shortening. Thus, the pre-ejection septal shortening during LBBB which occurs against low LV pressure, and therefore represents little work, would appear erroneously as a more substantial work if timing of aortic valve opening (AVO) was set prematurely. Similarly, the work represented by post-systolic shortening in ischaemic myocardium

would be overestimated if timing of aortic valve closure (AVC) was set too late. The error in timing of IVC and IVR, however, was minor as demonstrated by testing sensitivity to errors in timing of AVO and AVC (see Supplementary material online, *Appendix S2*). Strain by STE is dependent on image quality to be able to accurately track the speckles from frame to frame. Therefore, work analysis may not be feasible in all patients. Furthermore, in patients with valvular pathology such as aortic stenosis, the pressure gradient over the valve will invalidate peripheral systolic arterial pressure as an estimate of peak LV pressure, and in these patients, the use of the estimated non-invasive pressure does therefore not apply.

## Limitations

The use of a reference curve to define timing of peak systolic pressure is in principle a limitation of the estimated pressure curve method since patients have different timing of peak LV pressure and this may vary from time to time in a given patient. This might have been improved by using brachial artery tonometry or a similar method to define timing of peak pressure and the pressure profile during LV ejection. However, additional analysis described in Supplementary material online, *Appendix S2*, showed that accurate timing of true peak pressure did not really matter since the impact on work of under- or overestimating LV pressure during the first part of the LV ejection phase was essentially compensated for by the opposite effect during the last part. For detection of more subtle differences in regional work, however, the use of a tonometrically recorded pressure curve may be of value. Measured LVP data from the analysed subject was not excluded from the average curve, as doing so did not significantly alter the estimated LV pressure waveform.

Speckle-tracking echocardiography measures motion in the image plane while sonomicrometry measures motion of material points in the myocardium. Therefore, a misalignment of the ultrasound plane vs. the crystals may account for some of the discrepancies between the two measurements. When calculating area strain and curvature, we used circumferential and longitudinal measurements obtained from two separate 2D echocardiographic projections. This method assumes that the projections are orthogonal and misalignment is a potential source of error.

Fluorodeoxyglucose positron emission tomography assesses glucose metabolism and will show increased uptake in areas both with aerobic and anaerobic (ischaemia) metabolism. Therefore, in the present study, we included only patients with a normal coronary angiography and no history of coronary artery disease. The observed abnormal changes in LV glucose metabolism during LBBB are in keeping with previous findings.[15]

The sample size in the present study is small and further validation of the findings should therefore be performed in a larger cohort; however, the consistency of the data support our findings.

### Potential for clinical application

As suggested by previous studies,[12,16,17] analysis of cardiac mechanics and regional work during ventricular dyssynchrony may provide important insights into mechanisms of remodelling and LV dysfunction. During LBBB, the early-activated septal segments produce little or negative work, while the late-activated segments are hyperstretched by the early septal contraction, and therefore generate more work than normal segments.[8,12] The difference in intersegmental work distribution during LBBB is associated with differences in regional blood flow and oxygen demand and may also account for remodelling of the left ventricle.[6,15,17,18] A clinical method which can assess regional work is therefore likely to provide important insights into cardiac mechanics and may be useful when evaluating patients who are candidates for CRT.

Because the proposed method uses LVP as a surrogate for force, it does not reflect changes in force that result from individual differences in LV geometry, and therefore, comparison between hearts is difficult. The most important application of the method would be to compare work between segments in a given ventricle. Such insight might be used to explore how non-uniformity of work distribution contributes to LV remodelling. Furthermore, studies should be done to determine whether work distribution during LV dyssynchrony may be used to identify responders to CRT and serve as a means to optimize electrode placement. Similar information cannot be obtained by just measuring strain, as illustrated by septal pre-ejection shortening and post-systolic shortening in the ischaemic myocardium which represent substantial shortening, but little work since LV pressure is low.

## Conclusions

In the present study, we introduce a novel non-invasive method for LV pressure–strain analysis which may serve as a means to quantify regional myocardial work and may also provide information regarding metabolic demand. Assessing work distribution will give the clinician additional information when assessing patients with ischaemia and might be useful for selecting patients for CRT. Furthermore, work analysis may play an important part in optimizing CRT settings and improve responder rate. Further studies are needed to define the clinical role of the proposed method.

## Supplementary material

Supplementary material is available at *European Heart Journal* online.


## Acknowledgements

The expert technical assistance of Randi Moen Forfang with the PET studies is gratefully acknowledged.

## Funding

K.R., E.W.R., and O.G. were recipients of clinical research fellowships from the University of Oslo, Helse Sør-Øst, and The Norwegian Research Council, respectively.

**Conflict of interest**: none declared.


## References


1. Suga H. Total mechanical energy of a ventricle model and cardiac oxygen consumption. *Am J Physiol* 1979;**236**:H498–H505.

2. Takaoka H, Takeuchi M, Odake M, Yokoyama M. Assessment of myocardial oxygen consumption ($Vo_2$) and systolic pressure–volume area (PVA) in human hearts. *Eur Heart J* 1992;**13**(Suppl. E):85–90.
3. Hisano R, Cooper G. Correlation of force–length area with oxygen consumption in ferret papillary muscle. *Circ Res* 1987;**61**:318–328.
4. Tyberg JV, Forrester JS, Wyatt HL, Goldner SJ, Parmley WW, Swan HJ. An analysis of segmental ischemic dysfunction utilizing the pressure–length loop. *Circulation* 1974;**49**:748–754.
5. Forrester JS, Tyberg JV, Wyatt HL, Goldner S, Parmely WW, Swan HJ. Pressure–length loop: a new method for simultaneous measurement of segmental and total cardiac function. *J Appl Physiol* 1974;**37**:771–775.
6. Delhaas T, Arts T, Prinzen FW, Reneman RS. Regional fibre stress-fibre strain area as an estimate of regional blood flow and oxygen demand in the canine heart. *J Physiol* 1994;**477**(Pt 3):481–496.
7. Urheim S, Rabben SI, Skulstad H, Lyseggen E, Ihlen H, Smiseth OA. Regional myocardial work by strain Doppler echocardiography and LV pressure: a new method for quantifying myocardial function. *Am J Physiol Heart Circ Physiol* 2005;**288**:H2375–H2380.
8. Gjesdal O, Remme EW, Opdahl A, Skulstad H, Russell K, Kongsgaard E, Edvardsen T, Smiseth OA. Mechanisms of abnormal systolic motion of the interventricular septum during left bundle-branch block. *Circ Cardiovasc Imaging* 2011;**4**:264–273.
9. Martin WH, Jones RC, Delbeke D, Sandler MP. A simplified intravenous glucose loading protocol for fluorine-18 fluorodeoxyglucose cardiac single-photon emission tomography. *Eur J Nucl Med* 1997;**24**:1291–1297.
10. Bland JM, Altman DG. Agreement between methods of measurement with multiple observations per individual. *J Biopharm Stat* 2007;**17**:571–582.
11. Goto Y, Igarashi Y, Yasumura Y, Nozawa T, Futaki S, Hiramori K, Suga H. Integrated regional work equals total left ventricular work in regionally ischemic canine heart. *Am J Physiol Heart Circ Physiol* 1988;**254**:H894–H904.
12. Prinzen FW, Hunter WC, Wyman BT, McVeigh ER. Mapping of regional myocardial strain and work during ventricular pacing: experimental study using magnetic resonance imaging tagging. *J Am Coll Cardiol* 1999;**33**:1735–1742.
13. Skulstad H, Edvardsen T, Urheim S, Rabben SI, Stugaard M, Lyseggen E, Ihlen H, Smiseth OA. Postsystolic shortening in ischemic myocardium: active contraction or passive recoil? *Circulation* 2002;**106**:718–724.
14. Bergman BC, Tsvetkova T, Lowes B, Wolfel EE. Myocardial glucose and lactate metabolism during rest and atrial pacing in humans. *J Physiol* 2009;**587**(Pt 9):2087–2099.
15. Nowak B, Sinha AM, Schaefer WM, Koch KC, Kaiser HJ, Hanrath P, Buell U, Stellbrink C. Cardiac resynchronization therapy homogenizes myocardial glucose metabolism and perfusion in dilated cardiomyopathy and left bundle branch block. *J Am Coll Cardiol* 2003;**41**:1523–1528.
16. Prinzen FW, Cheriex EC, Delhaas T, van Oosterhout MFM, Arts T, Wellens HJJ, Reneman RS. Asymmetric thickness of the left ventricular wall resulting from asynchronous electric activation: a study in dogs with ventricular pacing and in patients with left bundle branch block. *Am Heart J* 1995;**130**:1045–1053.
17. van Oosterhout MF, Prinzen FW, Arts T, Schreuder JJ, Vanagt WY, Cleutjens JP, Reneman RS. Asynchronous electrical activation induces asymmetrical hypertrophy of the left ventricular wall. *Circulation* 1998;**98**:588–595.
18. Prinzen FW, Augustijn CH, Arts T, Allessie MA, Reneman RS. Redistribution of myocardial fiber strain and blood flow by asynchronous activation. *Am J Physiol* 1990;**259**(2 Pt 2):H300–H308.

# Paper 4